Decay of mass-separated ^{141}Cs to ^{141}Ba and systematics of $N=85$ isotones

H. Yamamoto, F. K. Wohn, K. Sistemich,* and A. Wolf†
Ames Laboratory and Department of Physics, Iowa State University, Ames, Iowa 50011

W. B. Walters and C. Chung
Department of Chemistry, University of Maryland, College Park, Maryland 20742

R. L. Gill, M. Shmid, and R. E. Chrien
Physics Department, Brookhaven National Laboratory, Upton, New York 11973

D. S. Brenner
Department of Chemistry, Clark University, Worcester, Massachusetts 01610
(Received 3 May 1982)

The decay of mass-separated ^{141}Cs produced in thermal neutron fission of ^{235}U was studied by x-ray and γ-ray spectroscopy. The level scheme deduced for the $N=85$ isotone ^{141}Ba differs substantially from previous level schemes. A new $\frac{7}{2}^-$ level at 55.0 keV was established as the second-excited state, completing the triplet of low-lying $\frac{3}{2}^-$, $\frac{5}{2}^-$, and $\frac{7}{2}^-$ states expected for this "quasi-$f_{7/2}$" nucleus. For transitions among these levels, values of $|\delta|(E2/M1)$ were deduced. Comparisons are made with level structures of other $N=85$ isotones. Systematic trends in energies of states characteristic of quasi-$f_{7/2}$ nuclei are discussed.

[RADIOACTIVITY ^{141}Cs [from ^{235}U(n,f)]; measured E_γ, I_γ, $\gamma\gamma$ coin., HpGe and Ge(Li) detectors; ^{141}Ba deduced levels, J, π, logft, $|\delta|$ ($E2/M1$). Mass-separated ^{141}Cs activity.]

I. INTRODUCTION

The odd-A $N=85$ isotones ^{147}Sm and ^{145}Nd have been described as "quasi-$f_{7/2}$" nuclei.[1] Cluster-vibration model or CVM (Ref. 1) calculations have been made by Paar *et al.*[2] for ^{147}Sm. Quasi-$f_{7/2}$ nuclei are characterized by a triplet of closely spaced low-lying $\frac{7}{2}^-$, $\frac{5}{2}^-$, and $\frac{3}{2}^-$ states. The $\frac{7}{2}^-$ state is the ground state for the $N=85$ isotones ^{149}Gd, ^{147}Sm, and ^{145}Nd, whereas the $\frac{3}{2}^-$ state becomes the ground state for the lighter isotones ^{143}Ce and ^{141}Ba. The spacing between the $\frac{7}{2}^-$ and $\frac{5}{2}^-$ levels decreases with decreasing proton number in going from ^{149}Gd to ^{143}Ce. Extrapolation of the smoothly varying level systematics to ^{141}Ba leads one to expect a nearly degenerate doublet of $\frac{7}{2}^-$ and $\frac{5}{2}^-$ levels. However, prior to the present study, there was no evidence for the existence of a low-lying $\frac{7}{2}^-$ level in ^{141}Ba.

Previous studies of the levels in ^{141}Ba were made from the decay of ^{141}Cs. There are no reaction data on levels in ^{141}Ba. Alvager *et al.*[3] and Tamai *et al.*[4] identified some of the stronger γ rays of the $A=141$ chain. The decay of mass-separated ^{141}Xe to levels in ^{141}Cs and the subsequent decay of ^{141}Cs to ^{141}Ba was reported by Otero *et al.*[5]; a level scheme for ^{141}Ba with a ($\frac{3}{2}^-$) ground state and a ($\frac{5}{2}^-$) state at 48.5 keV was proposed. A similar study by Cook and Talbert[6] yielded a preliminary decay scheme for ^{141}Cs which was included in the most recent $A=141$ evaluation by Tuli.[7] This study confirmed by the ($\frac{3}{2}^-$) ground state and the ($\frac{5}{2}^-$) state at 48.5 keV proposed in Ref. 5. Neither study proposed a low-lying $\frac{7}{2}^-$ level.

Additional information prior to the present study consisted of measurements via atomic hyperfine interactions of ground-state spins of $\frac{3}{2}$ for ^{141}Ba (Ref. 8) and $\frac{7}{2}$ for ^{141}Cs.[9] From spontaneous fission of ^{252}Cf, Clark *et al.*[10] reported a lifetime of 20 ± 7 ns for the 48.5-keV transition. From the β decay of ^{141}Cs, Morman *et al.*[11] found an upper limit of 3.4 ns for the lifetime of the 48.5-keV level. More re-

 ©1982 The American Physical Society

cently, laser spectroscopic methods have been extended to the neutron-rich odd-A Ba isotopes from ^{139}Ba to ^{145}Ba.[12] For the ground state of ^{141}Ba, a magnetic dipole moment $\mu = -0.4\ \mu_N$ and a spectroscopic electric quadrupole moment $Q_2^s = 0.6$ b have been deduced.[12]

The present study was done with mass-separated ^{141}Cs from the isotope separator on-line (ISOL) facility TRISTAN at Brookhaven National Laboratory. The initial objective of the study was to search for the expected low-lying $\frac{7}{2}^-$ state in ^{141}Ba. The search was successful, as our x-ray, γ-ray, and γ-γ coincidence data allowed us to construct a revised level scheme with a $\frac{7}{2}^-$ state at 55.0 keV which decays predominantly via a highly converted 6.5-keV $M1$ transition to the $\frac{5}{2}^-$ state at 48.5 keV.

Comparison of the level structures of quasi-$f_{7/2}$ levels in ^{141}Ba with levels of the same J^π in other $N=85$ isotones reveals smooth trends in the level energies with proton numbers. This comparison and interpretation of the level structures using the CVM treatment[1,2] are presented in the discussion section.

II. EXPERIMENTAL PROCEDURES

Radioactive sources of mass-separated ^{141}Cs were produced by the TRISTAN isotope separator facility on-line to the high flux beam reactor (HFBR) of the Brookhaven National Laboratory. Detailed descriptions of TRISTAN have been presented elsewhere.[13,14] Ion beams of Rb, Sr, Cs, Ba, Ce, and Pr isotopes are obtained from an integrated target ion-source system.[15] The target consists of ~ 5 g of ^{235}U adsorbed onto a graphite cloth cylinder inserted into a Ta cylinder of 3-cm length and 2-cm diameter. The target is located in a neutron flux of $\sim 1.5 \times 10^{10}$/cm^{2}s. The tantalum ion source has a Re ionizer on the inner surface of a 2-mm diameter exit tube. The source is heated by electron bombardment to $\sim 2000°$C. For the present study lower temperatures ($\sim 1200°$C) were used in order to reduce the Ba ionization efficiency relative to that of Cs. The $A = 141$ ions were deposited on the tape of a moving tape collector (MTC). The MTC made it possible to strongly enhance the 24.9-s ^{141}Cs activity over the 18.3-m ^{141}Ba activity.

A low-energy photon spectrometer (LEPS) with 0.55-keV FWHM at 122 keV, a HpGe detector with 1.6-keV FWHM at 1332 keV, and a large-volume Ge(Li) detector with 2.1-keV FWHM at 1332 keV were used in x-ray and γ-ray measurements. Singles measurements were made with HpGe and Ge(Li) detectors both 7 cm from the beam deposit spot and, during a subsequent run, with the LEPS detector located 5 cm from the deposition spot. Three-parameter γ-γ-t coincidence measurements were made with the HpGe and Ge(Li) detectors each 4 cm from the deposit spot.

Level lifetime measurements were made with a 2.5 cm$\times$2.5 cm plastic detector and a 2.5 cm $\times$ 1.3 cm NaI(Tl) detector both of which were attached to XP1021 fast photomultipliers. Start pulses for a TAC were derived by a constant fraction single channel analyzer using pulses from the anode of the photomultiplier of the plastic detector. Stop pulses were derived from a constant fraction discriminator using pulses from the anode of the photomultiplier of the NaI(Tl) detector. The TAC pulses were strobed by a gate signal from a timing single channel analyzer gating on pulses from the dynode of the photomultipler of the NaI(Tl) detector.

III. EXPERIMENTAL RESULTS

A. γ-ray singles

Figure 1 shows a spectrum obtained with the HpGe detector during a 25-s deposit and simultaneous counting period, after which the tape was moved and the cycle repeated. Figure 2 shows a low-energy x-ray and γ-ray spectrum obtained with the LEPS detector at a MTC time cycle of 0.6-s deposit followed by a 10-s counting period. Standard sources of ^{56}Co, ^{57}Co, ^{88}Y, ^{109}Cd, ^{113}Sn, ^{137}Cs, ^{139}Ce, ^{203}Hg, and ^{241}Am were used to calibrate x ray and γ-ray energies and intensities and to determine the nonlinearities of the detector systems. For the LEPS detector, the photopeak efficiency was obtained down to 4 keV by using K and L x rays as well as γ rays. The LEPS energy calibration was linear within ± 30 eV from 4 to 200 keV and the nonlinearity was determined to an accuracy of ± 5 eV.

Energies, intensities, and placements of the γ rays assigned to the decay of ^{141}Cs are given in Table I. Our energies and intensities agree well with those of Cook and Talbert.[6] We have assigned a total of 192 γ rays and placed 187 of these in the ^{141}Cs decay scheme. Table I contains 30 γ rays not reported by Cook and Talbert; most of these are doublets which were resolved either in singles or γ-gated spectra of the high-resolution HpGe detector. The peaks are

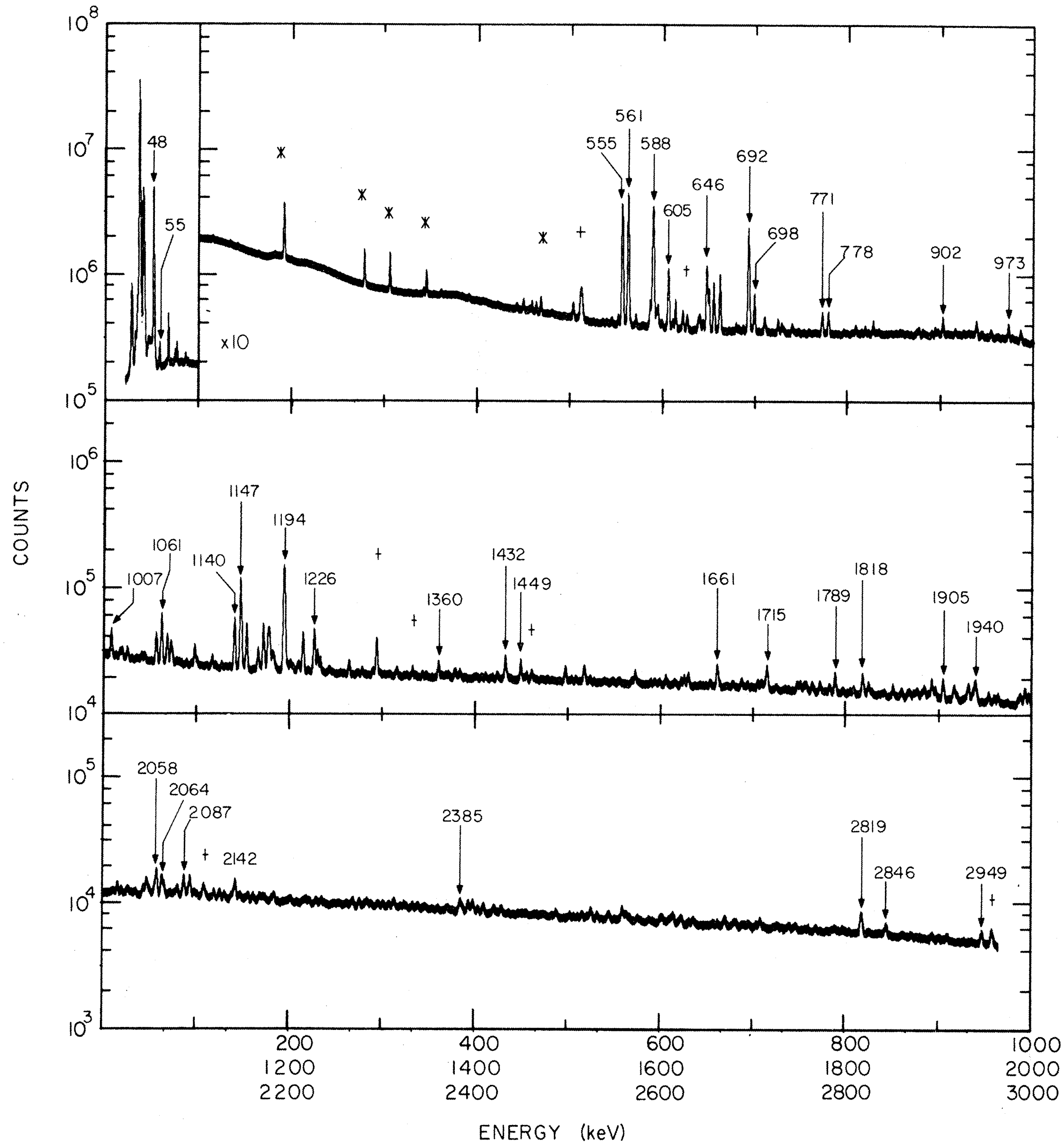

FIG. 1. $A=141$ γ spectrum with ^{141}Cs enhanced. Selected ^{141}Cs peaks labeled. ^{141}Ba and background peaks indicated by * and †, respectively.

of low intensity ($<1\%$ of 48-keV intensity). Cook and Talbert reported only four weak peaks that we did not observe. Otero *et al.*,[5] on the other hand, reported 141 γ rays in the ^{141}Cs decay; 57 of these 141 were either assigned to other $A=141$ isobars, observed only in background spectra, or not observed in the present study. Of the 84 γ rays reported by both Otero *et al.* and the present study, the γ-ray intensities are generally $\gtrsim 2\%$ of that of the 48-keV γ ray.

B. γ-γ coincidences

The γ-γ-t coincidence events of dimension $8192\times8192\times256$ were made with the HpGe and Ge(Li) detectors at 180° geometry. A total of 24×10^6 coincidence events were recorded on magnetic tape. Spectra in coincidence with selected peak, background, and time gates were reconstructed using the TRISTAN PDP 11/34 data analysis computer. (A complete description of the TRIS-

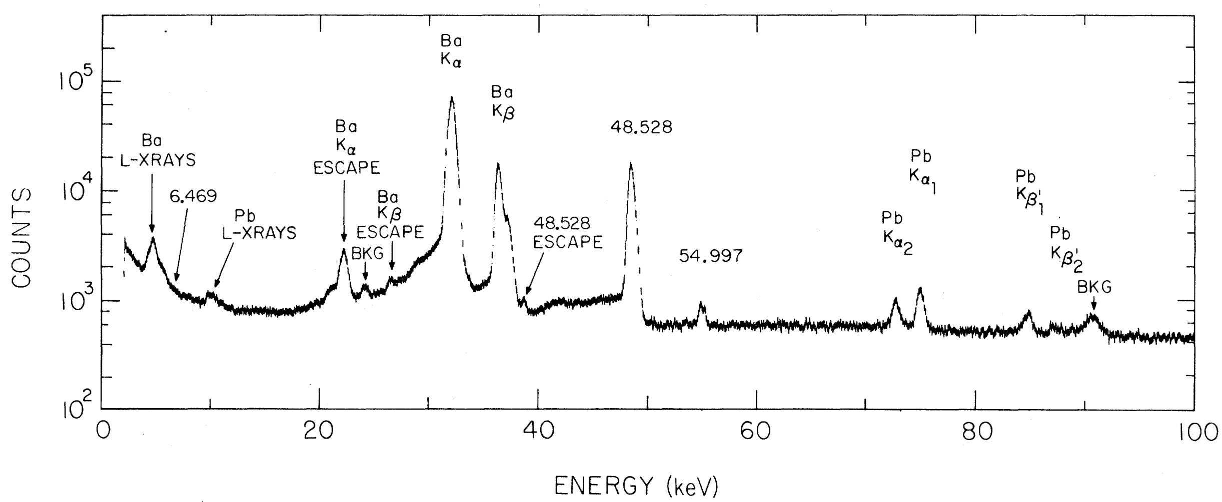

FIG. 2. γ and x rays observed in the decay of ^{141}Cs.

TAN data acquisition and analysis systems is given in Ref. 16.) A coincidence acceptance window of ~50 ns and an equal-width accidentials window, time shifted by ~150 ns, were used in the analyses. For the γ rays which form unresolved doublets, split peak gates were used and analyzed quantitatively to confirm the double placement of these γ rays in the decay scheme. For such γ rays the quantitative analyses of the split gates (and also gates on cascade γ rays populating or depopulating the levels involved) were used to determine the intensities of the two components of the doublet. The results of the coincidence analyses are shown in Table II.

Figure 3 shows gated spectra for the 48-, 555-, and 561-keV γ rays. The 48-keV gate reveals many coincident γ rays, in contrast to the study of Otero *et al.*,[5] who apparently had too low a coincidence efficiency at ~50 keV to observe these coincidences. The 555- and 561-keV gates show nearly identical spectra, as Fig. 3 and Table II indicate. This is evidence against the preliminary decay scheme of Cook and Talbert[6,7] in which both of these γ rays populate the first-excited state at 48.5 keV. The results of these gates indicate that both the 555- and 561-keV γ rays depopulate a level at 610 keV. This interpretation, which is supported by results from other gates, implies the existence of an intense 6.5-keV transition between a level at 55.0 keV and the 48.5-keV level. Twenty pairs of γ rays differing in energy by 6.5 keV were found to populate the 55.0- and 48.5-keV levels; seven of these pairs were intense enough to give coincidence confirmation (see Table II) of this interpretation. The 55.0-keV level is depopulated by both 55.0- and 6.5-keV transitions. The weak 55.0-keV gate supports this interpretation, as the 555-keV γ ray is seen in this gate, whereas the 561-keV γ is absent.

C. L x rays and 6.5-keV γ ray

The LEPS spectra were taken to measure the intensity and deduce the multipolarity of the 6.5-keV transition whose existence was implied by the γ-γ coincidence results. The LEPS data were also used to deduce the $E2/M1$ mixing in the 48.5-keV transition. Figure 2 shows the peaks of interest in the LEPS spectra. The L x rays and the 6.5-keV γ ray are shown in detail in Fig. 4. Figure 4(a) shows three pairs of L x rays, with one pair from each L subshell. The most intense x rays from each subshell were grouped into two peaks and the relative intensities of x rays from each subshell were held fixed to the theoretical values of Scofield.[17] x rays contributing $\lesssim 1\%$ of the subshell depopulation intensity were ignored. (The relative intensities of the K x rays were found to be in excellent agreement with the theoretical values of Scofield.)

The fit shown in Fig. 4 was made with the following constraints: (1) all peak centroids were held fixed since the energy nonlinearities had been determined to an accuracy of ± 5 eV, (2) relative intensities of all x rays depopulating a given L subshell were constrained to the values from Scofield,[17] (3) peak shape parameters were held fixed to values determined from spectra of the calibration standards used to determine photopeak efficiencies and

TABLE I. γ rays observed in the decay of ^{141}Cs.

Energy (keV)	Relative intensity	Placement (keV)	Energy (keV)	Relative intensity	Placement (keV)
6.469±0.050	20.5± 1.8	55- 48	1126.96±0.14	7.6± 0.5	1874- 747
48.528±0.008	1000 ±30	48- 0	1140.50±0.07	127 ±88	1195- 55
54.997±0.023	18.7± 1.5	55- 0	1147.00±0.11	240 ±25[a]	1195- 48
340.56 ±0.13	4.3± 0.3	1844-1503	1147.2 ±0.3	121 ±22[a]	1202- 55
441.28 ±0.14	4.0± 0.3	1690-1249	1153.64±0.07	112 ± 7	1202- 48
448.42 ±0.12	11.1± 0.7	1195- 747	1165.87±0.12	37.2± 2.2	1214- 48
501.98 ±0.12	15.4± 0.9	1249- 747	1171.55±0.11	112 ± 7	1226- 55
509.7 ±0.3[b]	22 ± 5	1256- 747	1176.67±0.12	80 ± 5	1231- 55
550.92 ±0.17	8.3± 1.2	1765-1214	1178.03±0.12	77 ± 5	1226- 48
555.15 ±0.06	470 ±30	610- 55	1181.16±0.14	29.8± 1.9	1229- 48
561.63 ±0.06	590 ±40	610- 48	1183.07±0.15	25.4± 1.7	1231- 48
569.79 ±0.15	12.4± 0.7	1765-1195	1194.02±0.11	500 ±30	1249- 55
585.39 ±0.11	34.2± 2.2	1195- 610	1195.63±0.18	32 ± 8	1942- 747
587.66 ±0.13	70 ± 7	1844-1256	1200.85±0.15	15.8± 1.2	2449-1249
588.79 ±0.07	480 ±30	643- 55	1210.0 ±0.3	10.4± 2.2	1853- 643
591.75 ±0.14	21.4± 1.6	1202- 610	1214.44±0.08	89 ± 6	1214- 0
605.28 ±0.06	129 ± 8	1249- 643	1226.43±0.11	106 ± 7	1226- 0
612.97 ±0.08	31 ± 3[a]	1256- 643	1229.95±0.12	42.5± 2.5	1229- 0
613.3 ±0.4	8 ± 4[a]	1844-1231	1232.96±0.13	25.3± 1.6	1942- 709
639.00 ±0.16	16.8± 1.6	1249- 610	1243.8 ±0.3	5.5± 0.8	1853- 610
642.60 ±0.14	9.8± 1.0	1844-1202	1263.93±0.12	20.9± 2.5	1874- 610
646.66 ±0.07	133 ±13	1256- 610	1277.91±0.17	8.5± 0.8	2394-1116
648.98 ±0.08	72 ± 5	1844-1195	1289.73±0.15	10.2± 0.8	
654.42 ±0.08	88 ± 6	709- 55	1315.27±0.20	17.4± 1.3	2062- 747
660.88 ±0.11	95 ±10	709- 48	1343.01±0.23	5.6± 0.6	2972-1629
692.04 ±0.06	380 ±22	747- 55	1360.30±0.17	29.7± 1.8	2107- 747
697.7 ±0.4	8 ± 3[a]	1341- 643	1383.39±0.22	11.4± 1.1	1432- 48
698.52 ±0.11	60 ± 5[a]	747- 48	1401.4 ±0.3	6.2± 0.9	3078-1677
709.42 ±0.15	19.1± 1.5	709- 0	1432.35±0.16	56 ± 3	1432- 0
728.09 ±0.14	11.2± 0.8	2274-1546	1449.02±0.16	41.3± 2.5	1503- 55
771.93 ±0.09	32.7± 1.9	827- 55	1452.6 ±0.3	6.1± 0.7	2062- 610
778.54 ±0.09	32.8± 1.9	827- 48	1455.28±0.22	11.4± 0.9	1503- 48
808.12 ±0.14	10.9± 0.8	2010-1202	1497.13±0.17	28.5± 1.7	2107- 610
827.00 ±0.12	19.3± 1.3	827- 0	1503.7 ±0.3	4.9± 0.6	1503- 0
894.07 ±0.16	9.9± 0.8	1503- 610	1517.57±0.18	35.6± 2.2	1572- 55
902.25 ±0.10	31.4± 1.9	1546- 643	1523.85±0.23	9.7± 0.9	1572- 48
938.34 ±0.16	19.0± 2.0	1765- 827	1539.2 ±0.3	4.5± 0.7	3043-1503
939.18 ±0.14	9.0± 2.0	1583- 643	1572.55±0.19	24.5± 1.5	1572- 0
954.10 ±0.14	11.3± 0.8	2010-1056	1574.8 ±0.3	6.7± 0.7	1629- 55
973.06 ±0.10	27.1± 1.6	1583- 610	1598.90±0.24	8.2± 0.8	1654- 55
985.98 ±0.13	19.1± 1.2	1629- 643	1605.72±0.21	16.3± 1.2	1654- 48
1007.76 ±0.12	54 ± 3	1056- 48	1625.76±0.20	18.5± 1.3	2874-1249
1017.31 ±0.14	12.3± 0.9	2274-1256	1630.11±0.18	25.2± 1.6	2274- 643
1019.58 ±0.13	14.5± 1.0	1629- 610	1654.10±0.23	6.6± 0.7	2363- 709
1025.03 ±0.13	16.9± 1.1	2274-1249	1661.51±0.16	50.4± 2.9	1709- 48
1043.96 ±0.14	9.6± 0.7	1654- 610	1678.89±0.21	15.2± 1.2	3120-1432
1056.24 ±0.11	59 ± 3	1056- 0	1709.5 ±0.3	15.5±1.1	1709- 0
1061.83 ±0.07	121 ± 7	1116- 55	1715.40±0.22	56 ±4	1764- 48
1066.88 ±0.24	8.8± 1.6	1677- 610	1738.7 ±0.3	4.6±0.7	2382- 643
1068.19 ±0.12	53 ± 4	1116- 48	1751.65±0.21	17.5±1.2	3334-1583
1071.94 ±0.13	37.1± 2.3	2274-1202	1758.1 ±0.3	15.1±1.2	2972-1214
1073.48 ±0.16	16.5± 1.3	1717- 643	1764.4 ±0.3	17.6±1.3	1764- 0
1097.59 ±0.11	37.8± 2.2	1844- 747	1772.74±0.25	18.8±1.3	2382- 610
1116.77 ±0.15	16.6± 1.3	1116- 0	1783.2 ±0.3	13.8±1.1	3031-1249

TABLE I. (Continued.)

Energy (keV)	Relative intensity	Placement (keV)	Energy (keV)	Relative intensity	Placement (keV)
1789.38±0.22	44.3±2.6	1844- 55	2615.5 ±0.3	14.4±1.2	3259- 643
1809.2 ±0.3	12.9±1.0	3004-1195	2637.5 ±0.3	11.4±1.0	3247- 610
1818.99±0.23	47.7±2.8	1874- 55	2671.7 ±0.3	15.6±1.1	3315- 643
1825.42±0.23	24.7±1.5	1874- 48	2709.8 ±0.3	13.1±1.5	3456- 747
1842.7 ±0.3	9.0±0.9	3099-1256	2728.6 ±0.4	7.9±0.8	4671-1942
1851.93±0.25	21.6±1.5	3078-1226	2819.56±0.21	27 ±3	2874- 55
1868.1 ±0.4	8.7±1.2	3099-1231	2846.21±0.25	16.3±1.1	3456- 610
1885.9 ±0.3	24.0±1.5	3087-1202	2949.49±0.20	18.4±1.2	3004- 55
1893.92±0.22	43.5±2.6	3120-1226	2976.8 ±0.3	16.3±1.2	3031- 55
1897.61±0.24	21.9±1.4	3111-1214	3032.4 ±0.3	4.3±1.6	3087- 55
1905.93±0.15	43.5±2.6	3120-1214	3038.87±0.25	29.9±2.1	3087- 48
1917.9 ±0.4	36.7±2.5	3120-1202	3056.9 ±0.3	23.8±1.7	3111- 55
1933.06±0.22	45 ±3	3189-1256	3071.93±0.22	63 ±4	3120- 48
1940.5 ±0.3	56 ±4	3189-1249	3077.72±0.25	35.1±2.1	3132- 55
1955.03±0.25	16.9±1.2	2010- 55	3098.6 ±0.3	10.7±1.0	4671-1572
1961.2 ±0.3	10.6±0.8	2010- 48	3115.32±0.23	41.1±2.6	3170- 55
1965.1 ±0.3	13.5±1.0	4239-2274	3120.5 ±0.3	16.4±1.2	3120- 0
1989.2 ±0.3	18.3±1.4		3132.5 ±0.4	23 ±3	4364-1231
1994.19±0.23	35.2±2.1	3189-1195	3134.4 ±0.4	21 ±3	3189- 55
1998.34±0.19	21.1±1.4	3247-1249	3169.1 ±0.3	11.2±1.0	4364-1195
2044.1 ±0.3	19.3±1.6	3273-1229	3183.1 ±0.3	11.8±1.0	4239-1056
2047.58±0.25	33.4±2.4	3243-1195	3188.6 ±0.7	3.5±1.0	3243- 55
2052.4 ±0.4	5.3±0.6	2107- 55	3192.2 ±0.3	41 ±5	3247- 55
2056.8 ±0.6	15 ±3	3259-1202	3194.4 ±0.4	19 ±5	3243- 48
2058.50±0.23	56 ±4	2107- 48	3204.3 ±0.3	9.6±0.9	3259- 55
2064.08±0.24	41.7±2.3	3120-1056	3218.2 ±0.4	5.3±0.7	3273- 55
2066.7 ±0.3	22.4±1.7	3315-1249	3224.9 ±0.3	20.5±1.5	3273- 48
2087.81±0.22	45.5±2.7	2142- 55	3238.2 ±0.4	4.8±0.6	4671-1432
2094.35±0.23	45.1±2.7	2142- 48	3252.24±0.25	21.1±1.4	
2139.6 ±0.3	4.3±1.3	3334-1195	3260.2 ±0.4	13.7±1.7	3315- 55
2142.83±0.23	42.5±2.6	2142- 0	3273.1 ±0.4	15.5±1.2	3273- 0
2327.8 ±0.6	4.0±1.0	2382- 55	3303.8 ±0.3	7.4±1.2	4533-1229
2385.5 ±0.3	20.5±1.6	3441-1056	3312.9 ±0.3	10.4±1.0	4544-1231
2387.9 ±0.4	9.8±1.2	3031- 643	3331.2 ±0.3	22.1±1.6	4533-1202
2394.40±0.25	20.5±1.3	2394- 0	3349.4 ±0.3	15.2±1.2	4544-1195
2399.14±0.25	23.3±1.5	3043- 643	3376.9 ±0.3	9.8±0.9	3431- 55
2410.9 ±0.3	16.4±1.2	3120- 709	3382.9 ±0.4	4.9±0.6	3431- 48
2489.3 ±0.3[c]	10.4±1.3	3099- 610	3395.6 ±0.9	3.0±1.3	4591-1195
2489.3 ±0.3[c]	10.4±1.3	3132- 643	3416.5 ±0.5	3.3±0.6	4533-1116
2503.8 ±0.4	5.7±0.8		3474.3 ±0.3	7.3±0.7	4591-1116
2533.5 ±0.3	8.4±0.9	3243- 709	3494.0 ±0.3	4.2±0.4	
2545.6 ±0.6	7 ±3	3189- 643	3529.2 ±0.4	3.3±0.5	4239- 709
2564.4 ±0.4	13.7±1.1	3273- 709			

[a]Total intensity of doublet split according to coincidence results.
[b]Peak seen only in coincidence spectra.
[c]Can be placed twice in level scheme.

energy nonlinearities, (4) the only free parameters in the fit were the intensity of the 6.5-keV γ ray (taken as pure $M1$ for reasons discussed in detail later) and the $E2/M1$ mixing ratio $|\delta|$ of the 48.5-keV transition. Figure 4(b) shows the three types of contributions to the total fit. In order of decreasing intensity, they are the following: (1) the 6.5-keV γ ray and the L x rays due to its internal conversion of $M1$ multipolarity, (2) the direct contributions due to L internal conversion for the $M1$ component of the

TABLE II. γ-γ coincidence results in the decay of ^{141}Cs.

Gate (keV)	Coincident γ rays[a] (keV)
48	(488), 501, 555, 561, (569), 585, 588, 605, 612, 646, 648, 654, 660, 692, 698, (902), (939), (954), (973), 1007, 1061, 1068, 1071, (1097), 1140, 1147.0, 1147.2, 1153, 1165, 1171, 1178, 1181, 1194, (1263), (1360), 1449, 1497, 1517, (1630), 1661, 1715, 1789, 1818, (1905), 1917, 1933, 1940, 1994, (2047), 2058, 2087, (2094), (2615), 2819, 2846, 2976, (3038), 3071, 3077, 3098, 3115, 3134, 3192, 3194, 3224, (3252), 3331
55	555, 588, (692), 1140, (1147.2), 1194
501	(48), 692, 698
555	48, (55), 585, 587, 591, 639, 646, 894, 973, 1017, 1019, 1043, 1066, 1263, (1452), 1497, (1772), 1933, (2637), (2846)
561	48, 585, 587, 591, 639, 646, 894, 973, 1017, 1019, (1043), 1066, 1263, 1497, (1772), 1933, (2637), (2846)
569	1140, 1147.0
585	48, 555, 561, 648, (1994), (2047)
587 + 588	48, 509, 555, 561, 587, 588, 605, 612, 646, 692, 697, (698), 902, 939, 985, 1073, 1210, 1630, 2387, 2399, 2545, 2615, 2671
591	555, 561
605	48, 588, 1025, 1200, 1625, 1940, 1998
612 + 613	48, 587, 588, 1176
639	555, 561
642	(1147.2), (1153)
646	48, 555, 561, 587, 1017, 1933
648	48, 448, (555), (561), 585, 1140, 1147.0
654	48, 1232, (1654), 2410, (2533), 2564, (2728)
660	48, 1232, 1654, 2410, (2533), 2564, (2728)
692	48, 448, 501, 509, (587), 1097, 1126, 1195, 1315, 1360
697 + 698	48, 448, 501, 509, 588, 1097, 1126, 1195, (1315), 1360
709	None
728	588, 902
771	938
778	(48), 938
827	938
894	48, 340, 555, 561
902	588, 728
938 + 939	(588), 771, 778, 827
973	551, 561
1007	(48), 954, 2064, 2385
1017	555, 561, (588), (612), 646
1019	555, 561
1025	(555), (561), (588), 605, 639, 1194
1056	954, 2064, 2385
1061	(48), 1277
1066	555, 561
1068	48, (1277)
1071	591, 1147.2, 1153
1073	588
1097	48, 692, 698
1116	None
1140	48, 569, 648, (1809), 1994, 2047, (2139)
1147.0 + 1147.2	48, 569, 648, 1071, 1809, (1885), 1917, 1994, 2047, 2056, 2139
1153	48, 1071, 1917, 2056
1165	48, 550, 1897, 1905
1171	48, 1893
1176	48, 613

TABLE II. (Continued.)

Gate (keV)	Coincident γ rays[a] (keV)
1178	48, (1851), 1893
1181	(48)
1194 + 1195	48, 441, 692, (698), 1025, 1200, 1625, 1783, 1940, 1998, 2066
1210	588
1214	550, 1758, 1897, 1905
1226	1851, 1893
1229	None
1232	48, 654, 660, 709
1263	(48), 555, 561
1315	692, 698
1360	692, 698
1432	1687
1449	(48), 340
1497	(48), 555, 561
1517	(48)
1523	(48)
1572	None
1605	(48)
1625	605, 1194
1630	588
1661	None
1715	(48)
1772	(555), (561)
1789	(48)
1818	(48)
1851	48, 1171, 1178, 1226
1885	(48), (1147.2)
1893	(48), 1171, 1178, 1226
1905	1165, 1214
1917	(48), 1147.2, 1153
1933	555, 561, (588), 612, 646
1940	48, 501, 588, 605, 1194
1994	(48), (555), (561), 585, 1140, 1147.0
1998	(501), (588), 605, (692), 1194
2047	1140, 1147.0
2056	1147.2, 1153
2058	48
2064	1007, 1056
2066	48, 605, 1194
2094	(48)
2139	1147.0
2142	None
2385	1007, 1056
2387	588
2399	(48), 588
2846	48, 555, 561
3038	48
3071	48
3077	48
3115	48
3134	48
3192	48
3224	48
3331	48

[a]Uncertain coincidences shown in parentheses.

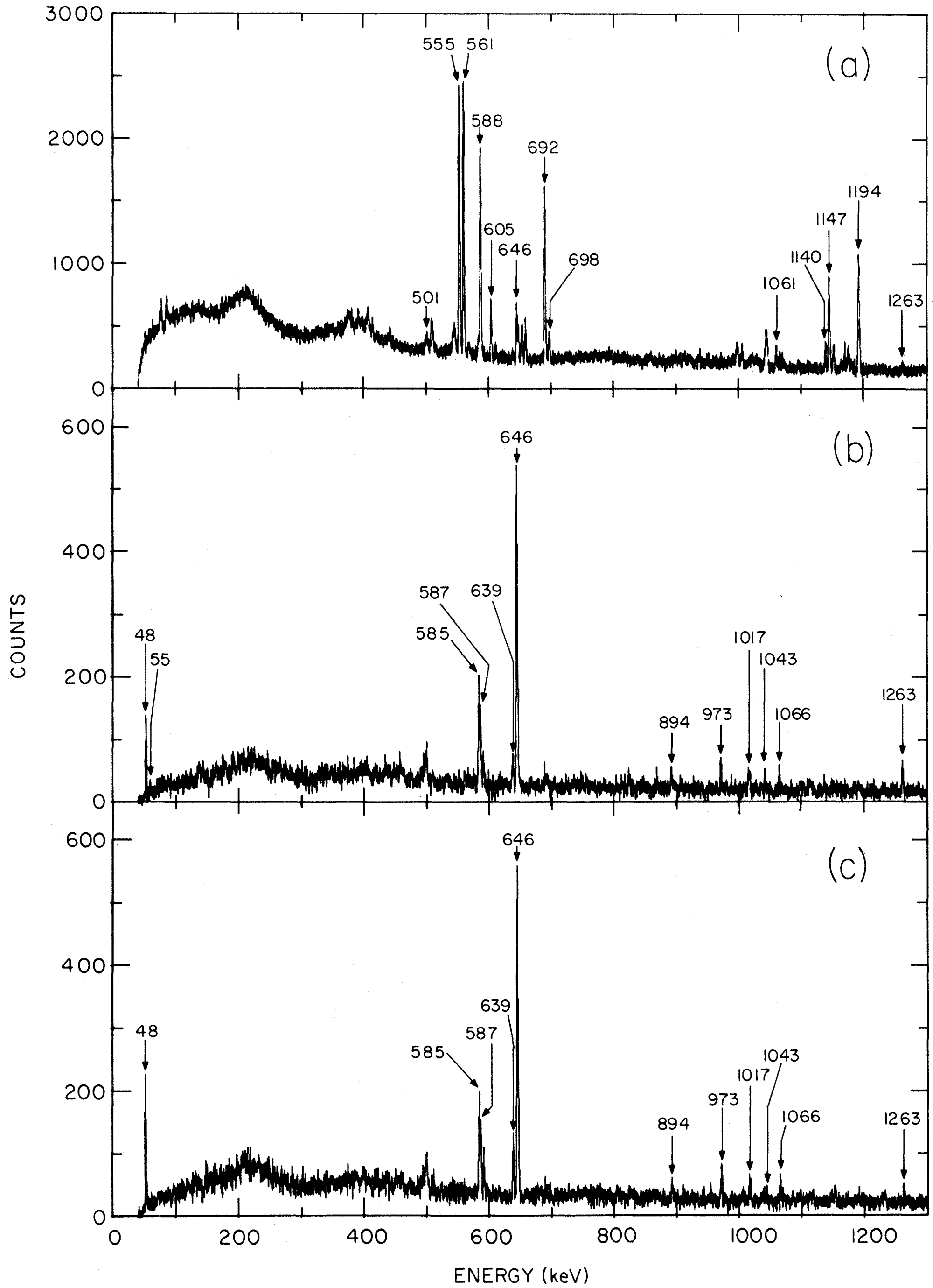

FIG. 3. Coincidence spectra, corrected for Compton events, for gates on γ rays of energy (a) 48.5 keV, (b) 555.1 keV, and (c) 561.6 keV.

48.5 keV and the pure $E2$ 55.0-keV transitions, plus the indirect contributions from filling K-shell vacancies due to K internal conversion of these two transitions, and (3) the direct contributions due to L internal conversion for the $E2$ component of the 48.5-keV transition. The fit showed that the 6.5-keV transition contributes 55% of the total L x-ray intensity and the 48.5-keV $E2$ component contri-

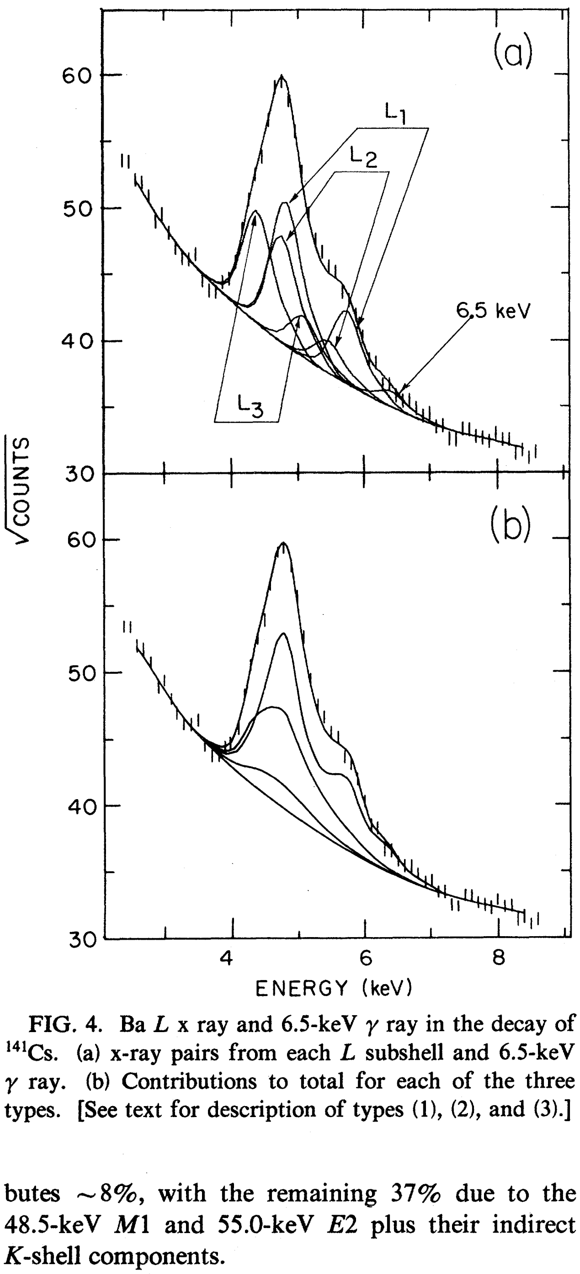

FIG. 4. Ba L x ray and 6.5-keV γ ray in the decay of ^{141}Cs. (a) x-ray pairs from each L subshell and 6.5-keV γ ray. (b) Contributions to total for each of the three types. [See text for description of types (1), (2), and (3).]

butes ~8%, with the remaining 37% due to the 48.5-keV $M1$ and 55.0-keV $E2$ plus their indirect K-shell components.

In fitting the L x-ray multiplet, use was made of Ba internal conversion coefficients from Rösel *et al.*,[18] which are given in Table III. Values for x-ray fluorescent yields, L-subshell Coster-Kronig transition probabilities, and indirect L-subshell vacancies caused by filing K-shell vacancies were obtained from the review paper of Bambynek *et al.*[19] Primary L subshell vacancies in ^{141}Cs decay are produced by internal conversion in the K and L shells; altered vacancies take into account the subsequent additional vacancies due to Coster-Kronig transitions within the L subshell. The intensities of x rays from each L subshell are given by the product of subshell fluorescent yield and altered subshell vacancy. Detailed descriptions of the quantities involved and their relationships are given in Ref. 19. Each altered vacancy was written as a sum of three terms, corresponding to the three contributions shown in Fig. 4(b) and described in the preceding paragraph. (It should be noted here that the same x-ray parameters and analysis method were used in analyzing the L x rays from the decay of ^{137}Cs; good agreement with accepted values was obtained for the L-subshell x-ray intensities.)

In the present case, note that the near equality of the α_K values for $M1$ and $E2$ at 48.5 keV implies that the K-shell vacancy contribution to L x rays is very insensitive to the $E2/M1$ mixing in the 48.5-keV transition. This implies that the intensity of the K x rays cannot be used to determine the 48.5-keV $E2/M1$ mixing. (Our experimental K x-ray intensity yields an α_K value of 7.03 ± 0.18 for the 48.5-keV transition, which is more precise than the value of 6.6 ± 0.9 of Otero *et al.*,[5] yet cannot distinguish between $M1$ and $E2$.)

The two-parameter fit shown in Fig. 4 resulted in the 6.5-keV γ-ray intensity of 20.5 ± 1.8 given in Table I and an $E2/M1$ mixing ratio $|\delta| = 0.36 \pm 0.11$ for the 48.5-keV transition; the uncertainties include the effects of uncertainties in the x-ray parameters used in the analysis. The L_1 subshell x rays are dominated by the 6.5-keV transition because of its large α_{L1} value; these L_1 x rays are

TABLE III. Internal conversion coefficients.

Energy (keV)	Multipolarity	α_k	α_{L1}	α_{L2}	α_{L3}	α_{total}
6.5	$M1$	0	342	32.2	7.5	482
6.5	$E2$	0	3.3×10^3	1.5×10^5	2.3×10^5	4.8×10^5
48.5	$M1$	7.01	0.87	0.07	0.02	8.23
48.5	$E2$	7.08	0.64	6.94	9.26	28.4
55.0	$E2$	5.76	0.50	3.81	4.84	17.4

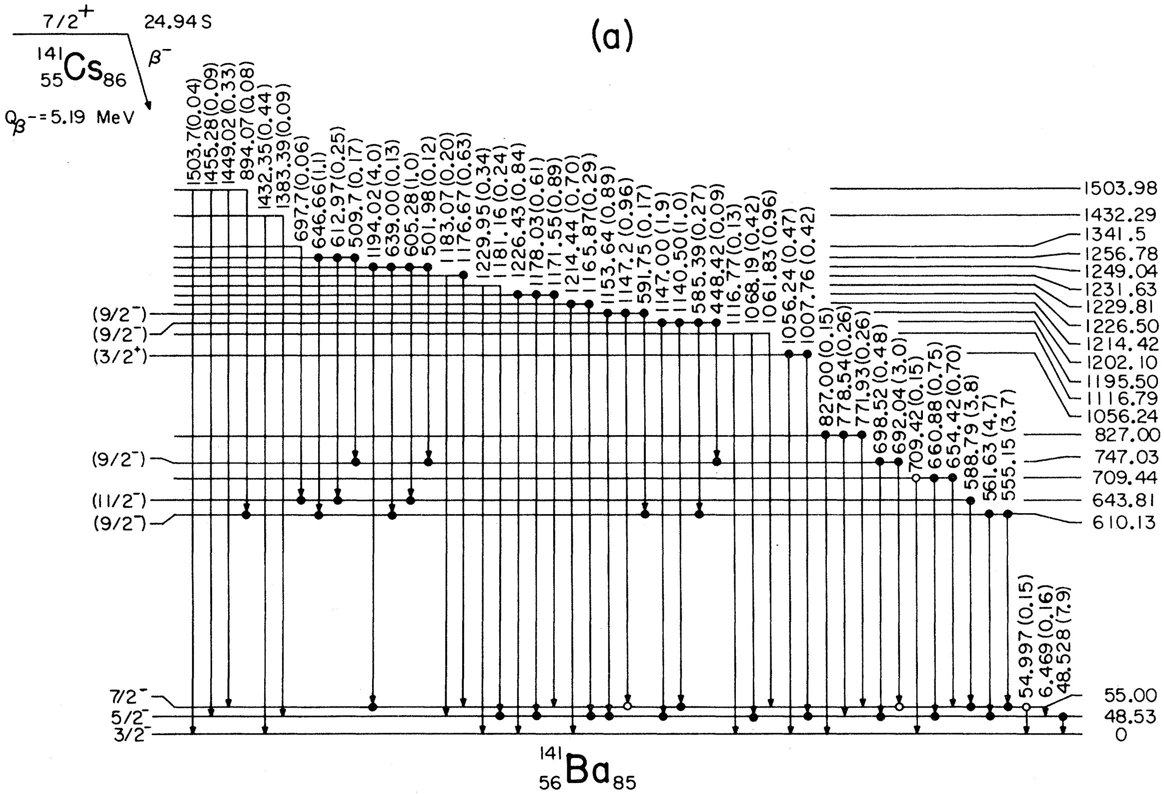

FIG. 5. Decay scheme for decay of ^{141}Cs to ^{141}Ba. Definite (filled circle) and less certain (open circle) coincidence shown at transition initial and final points. Selected J^{π} values indicated; see Table IV for complete list of J^{π} values. Intensities for γ transitions are indicated per 100 decays. (a) Levels to 1503 keV; (b) levels from 1546 to 2107 keV; (c) levels from 2142 to 3170 keV; (d) levels from 3189 to 4671 keV. Note that not all lower levels are shown in (b), (c), and (d).

nearly independent of the $E2/M1$ mixing of the 48.5-keV transition due to the nearly equal values of α_{L1} at 48.5 keV. A four-parameter fit in which the 6.5-keV γ-ray intensity and the three L_i x-ray pairs were free to vary in intensity was also made; this fit yielded the values 20 ± 5 for the 6.5-keV γ-ray intensity and $|\delta| = 0.40\pm0.30$ for the $E2/M1$ mixing ratio of the 48.5-keV transition. Although these values agree with the more highly constrained two-parameter fit values, the latter values are more reliable since the strength of the 6.5-keV transition is far better defined by the x rays than by the weaker γ ray. As discussed in the following section, our preferred values of $I_{\gamma} = 20.5\pm1.8$ and $|\delta| = 0.36\pm0.11$ satisfy the constraints imposed by the decay scheme.

D. Level lifetime measurements

The level-lifetime measurements system was tested using ^{22}Na annihilation radiation, ^{133}Ba decay γ rays, and ^{152}Er decay γ rays. The FWHM of the unstrobed prompt peak for the annihilation radiation was 0.8 ns; the slope on the plastic side of the peak was equivalent to a 0.6-ns half-life. The 6-ns half-life of the 80-keV level in ^{133}Cs was easily observed with the strobe window on the NaI(Tl) detector set to accept γ rays above 100 keV and showing the 6-ns half-life on the start (i.e., plastic) side. Alternatively, the gate could also be set on either the 80-keV region or the 40-keV region containing Cs x rays and showing the 6-ns half-life on the stop side. The 1.2 ns half-life of the 121-keV level in ^{152}Sm could not be measured with this system. With the strobe set high in the NaI(Tl) detector a 1.5-ns half-life was observed in the plastic detector whereas a 3-ns half-life was observed when the strobe gate was set on the 121-keV region or on the region of the Sm x rays.

For the ^{141}Cs decay, the strobe gate was set on the 200−350 keV region of Compton γ rays from the 555- and 561-keV γ rays. A half-life of 5.0 ± 0.1 ns was observed for the low-lying unresolved Ba x rays, and the 48- and 55-keV γ rays that would be

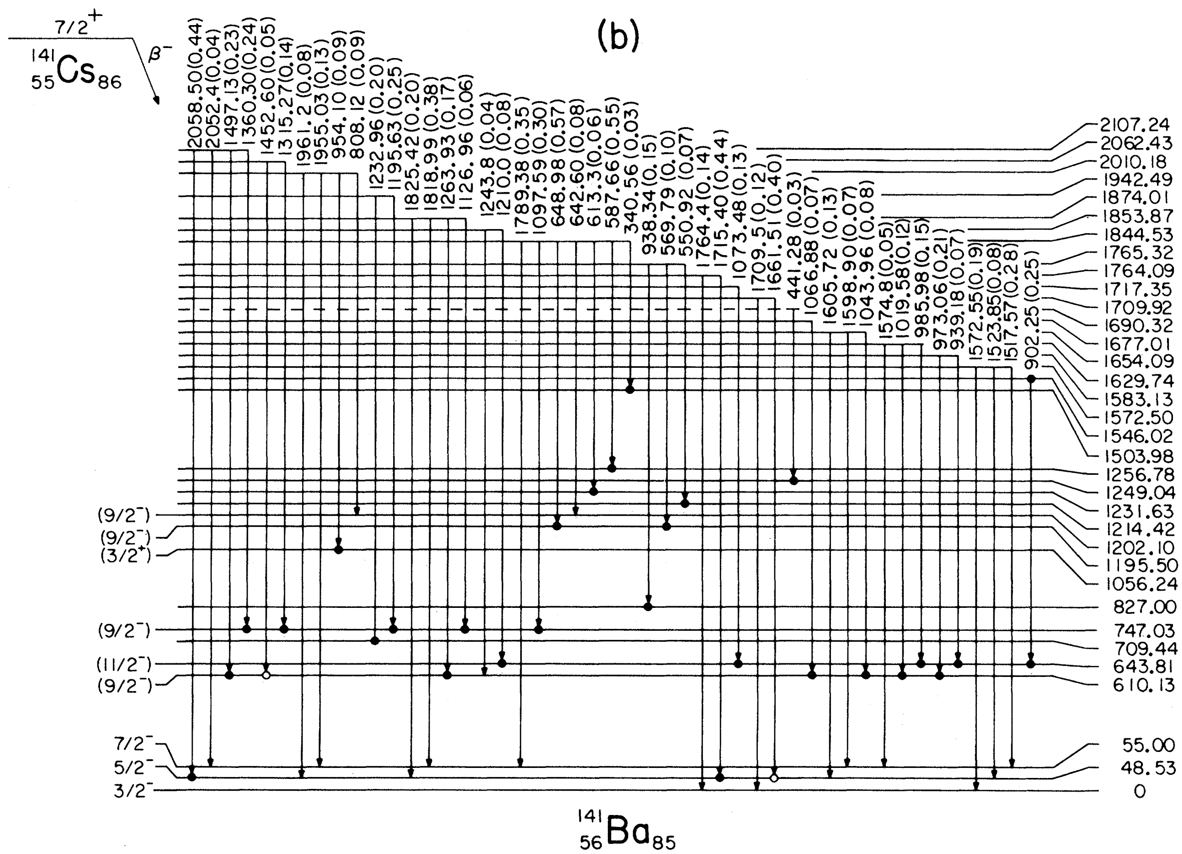

FIG. 5. (*Continued*.)

efficiently stopped by the small plastic detector. Since it was not possible to resolve the 555- and 561-keV γ rays with our plastic-NaI system, we cannot determine the individual lifetimes of the two levels at 48.5 and 55.0 keV.

IV. DECAY SCHEME

The ^{141}Cs decay scheme is shown in Fig. 5. Definite coincidences are shown by filled circles and less certain coincidences by open circles. The Q_β value of 5.19 MeV used in our log*ft* calculations is a weighted average of the measured values 5.187 ± 0.025 MeV (Ref. 20) and 5.20 ± 0.08 MeV.[21] Zero β branching to the ground state of ^{141}Ba was assumed in calculating log*ft* values. This assumption leads to an absolute intensity of 7.9% for the 48.5-keV γ ray, in excellent agreement with the value of 7.9% obtained in the study of Otero *et al.*[5] Level energy, β branching, and log*ft* values are given in Table IV.

A. Low-lying $\frac{3}{2}^-$, $\frac{5}{2}^-$, $\frac{7}{2}^-$ levels

The new level at 55.0 keV has a significant impact on the low-energy β branchings. The previous studies, Refs. 5 and 6, respectively, deduced β branches of $\sim 70\%$ and 60% to the $\frac{5}{2}^-$ level at 48.5 keV, in reasonable agreement with our total β branching of 57% to the two levels at 48.5 and 55.0 keV. However, all of this branching can now be attributed to the 55.0-keV level, with essentially zero branching to the 48.5-keV level. The upper limit of $<4\%$ for the β branch to the 48.5-keV level results primarily from the uncertainties in the 6.5-keV γ-ray intensity and the 48.5-keV α value. With these uncertainties taken into account, the 48.5-keV level has a population intensity of $(93.8 \pm 4.5)\%$ and a depopulation intensity of $(92.8 \pm 0.4)\%$, yielding a β branch of $(-1.0 \pm 4.5)\%$. The result that the $\frac{7}{2}^-$ level receives all the β branching to the low-energy triplet was also found for the β decay of ^{145}Pr (also $\frac{7}{2}^+$) to the $N=85$ isotone ^{145}Nd.[22] The

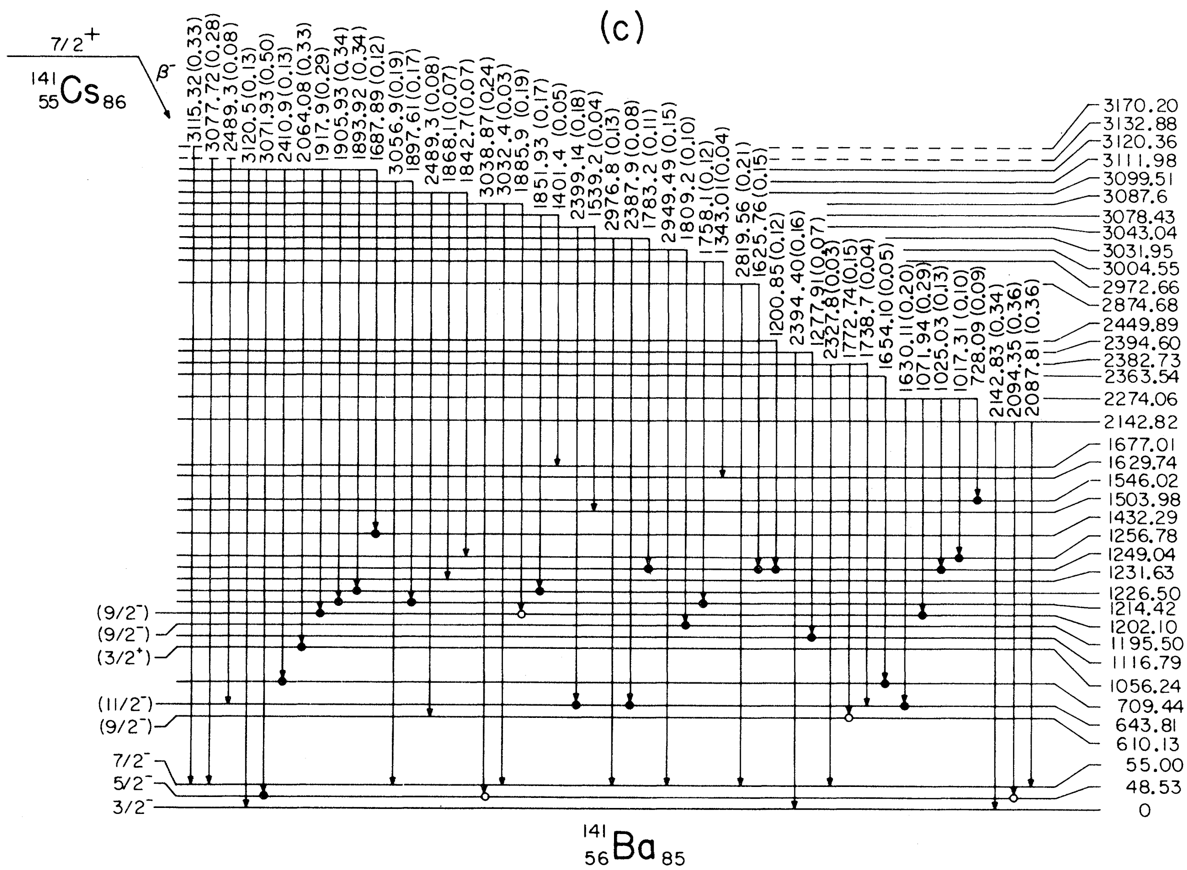

FIG. 5. (*Continued.*)

branching to the low-energy triplet has not been clarified for the neighboring $N=85$ isotone ^{143}Ce.[23]

The relative intensity of 20.5 for the 6.5-keV γ ray, which was determined from fitting the L x rays, is essentially the maximum intensity permitted by the decay scheme and the assumed pure $M1$ multipolarity of this γ ray. Since the transition connects levels with J^π values of $\frac{7}{2}^-$ and $\frac{5}{2}^-$, an $E2$ component cannot be ruled out. (A Weisskopf $E2$ lifetime estimate of ~ 2 μs implies a very small $E2$ component, even with an $E2$ enhancement of 10^2-10^3 considered.) The best direct evidence for a negligible $E2$ component in the 6.5-keV transition comes from the L x rays and is related to the enormous difference between α_L values for $M1$ and $E2$ at this low energy (see Table III). For $M1$, $\alpha_{L1} \gg \alpha_{L2,3}$ whereas for $E2$, $\alpha_{L1} \ll \alpha_{L2,3}$. The L_1 x rays are due primarily ($\sim 86\%$) to the 6.5-keV direct L_1 interval conversion because the 48.5- and 55.0-keV transitions have a minimal effect, either through direct L or indirect K internal conversion, on the L_1 subshell. If the 6.5-keV transition had a significant $E2$ component, then the L_1 x rays would be much weaker than the L_2 and L_3 x rays; Fig. 4 clearly shows that this is not the case. Furthermore, a significant $E2$ component for the 6.5-keV transition, due to the large α_{total} for $E2$, would result in far more intensity populating the 48.5-keV level than depopulating it. Thus both the L x rays and the decay scheme indicate essentially pure $M1$ multipolarity for the 6.5-keV transition.

The α_{total} value of 10.6 ± 1.4 for the 48.5-keV transition corresponds to an $E2/M1$ mixing ratio $|\delta| = 0.36 \pm 0.11$. Pure $M1$ and $E2$ α_{total} values from Table III were used for the 6.5- and 55.0-keV transitions, respectively. With these values, the 6.5-keV transition comprises 97% of the depopulation intensity of the 55.0-keV level. Thus the relative intensities of the 555- and 561-keV γ rays in the 48.5-keV gate are essentially identical to their relative intensities in singles, as observed for this pair and other γ-ray pairs with $\Delta E = 6.5$ keV. This observation implies a short ($\lesssim 10^{-8}$ s) lifetime for the levels at 48.5 and 55.0 keV, as was verified by our subsequent measurement of 5.0 ns.

Our 5.0 ns result for the 48.5- and 55.0-keV levels

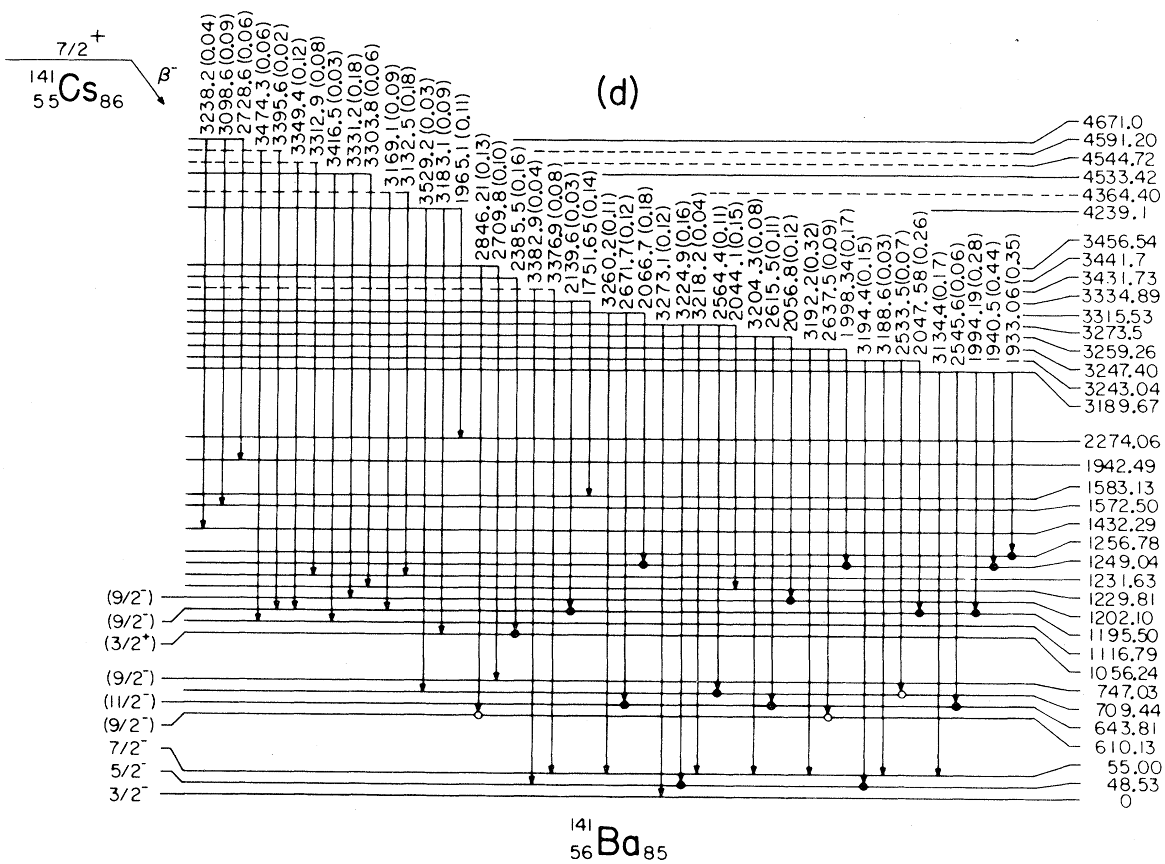

FIG. 5. (*Continued.*)

in ^{141}Ba can be compared with lifetimes of the analogous levels in other $N=85$ isotones. Significant $E2$ enhancements and $M1$ hindrances can be expected relative to Weisskopf single-particle estimates. Using known lifetimes and mixing ratios for transitions among the low-lying $\frac{3}{2}^-$, $\frac{5}{2}^-$, and $\frac{7}{2}^-$ levels in the $N=85$ isotones ^{145}Nd, ^{147}Sm, and ^{149}Gd (Refs. 22, 24, and 25, respectively), enhancement and hindrance factors can be calculated. $E2$ enhancements in the range $10-10^2$ were found for five transitions and $M1$ hindrances in the range 10^2-10^3 were found for four transitions. Assuming enhancements or hindrances in such ranges also for the corresponding transitions in ^{141}Ba, the lifetimes of the 48.5- and 55.0-keV levels are then "expected" to be of the order of a few ns. This agreement with expectations for ^{141}Ba lends support to the assertion that the low-lying triplets in all $N=85$ isotones have similar structure.

The decay scheme in Fig. 5 indicates definite J^π values for the ^{141}Cs ground state and the three low-energy states in ^{141}Ba. These assignments can be justified as follows. The ground-state spins were determined experimentally[8,9] and the parity assignments are expected from either the spherical shell model or neighboring odd-A Cs isotopes and $N=83$, 85,87 isotones. With a $\frac{3}{2}^-$ ground state in ^{141}Ba, $M1$ multipolarity for the 48.5-keV transition limits J^π to $\frac{1}{2}^-$, $\frac{3}{2}^-$, or $\frac{5}{2}^-$ for the 48.5-keV level. The logft value of 6.1 for the β branch to the 55.0-keV level limits its J^π to $\frac{5}{2}^\pm$, $\frac{7}{2}^\pm$, or $\frac{9}{2}^\pm$, as only allowed or first-forbidden nonunique β decays can have log$ft=6.1$.[26] With $M1$ for the 6.5-keV transition, the preceding J^π ranges are reduced to $\frac{3}{2}^-$, $\frac{5}{2}^-$ at 48.5 keV and $\frac{5}{2}^-$, $\frac{7}{2}^-$ at 55.0 keV. Unique choices of $\frac{5}{2}^-$ at 48.5 keV and $\frac{7}{2}^-$ at 55.0 keV are strongly implied by the intensity ratio of 0.035 for the 55.0- and 6.5-keV transitions. If the 55.0-keV level were $\frac{5}{2}^-$, then the 55.0-keV transition could be $M1$ and thus would be expected to be more intense than the 6.5-keV transition by a factor of $\sim 10^3$, assuming similar $M1$ hindrances for both transitions. Only if the 55.0-keV transition is restricted to pure $E2$ (by the $\frac{7}{2}^-$ assignment) can the observed intensity ratio make sense. ($M1$ hindrances and $E2$ enhancements would have to differ

TABLE IV. Beta branching and logft values for ^{141}Cs decay.

Level energy (keV)	β branching (%)	Logft	J^π
0.0	0		$\frac{3}{2}^-$
48.53±0.02	<4	>7.2	$\frac{5}{2}^-$
55.00±0.04	57. ±4	6.1	$\frac{7}{2}^-$
610.13±0.07	5.3 ±0.5	6.9	$(\frac{9}{2}^-)$
643.81±0.07	1.0 ±0.3	7.6	$(\frac{11}{2}^-)$
709.44±0.08	1.0 ±0.1	7.6	$\frac{3}{2}^-, \frac{5}{2}^-, \frac{7}{2}^-$
747.03±0.06	2.0 ±0.2	7.3	$(\frac{9}{2}^-)$
827.00±0.06	0.52±0.04	7.8	$\frac{3}{2}^-, \frac{5}{2}^-, \frac{7}{2}^-$
1056.24±0.07	0.22±0.05	8.1	$(\frac{3}{2}^+)$
1116.79±0.07	1.4 ±0.1	7.3	$\frac{3}{2}^-, \frac{5}{2}^-, \frac{7}{2}^-$
1195.50±0.06	1.7 ±0.2	7.2	$(\frac{9}{2}^-)$
1202.10±0.13	0.8 ±0.2	7.5	$(\frac{9}{2}^-)$
1214.42±0.06	0.3 ±0.1	7.9	$(\frac{1}{2}^-, \frac{3}{2}^+)$
1226.50±0.06	1.8 ±0.1	7.1	$\frac{3}{2}^-, \frac{5}{2}, \frac{7}{2}^-$
1229.81±0.15	0.36±0.04	7.8	$(\frac{3}{2}^+)$
1231.63±0.12	0.4 ±0.1	7.7	$(\frac{9}{2}^-)$
1249.04±0.07	3.9 ±0.3	6.8	$\frac{9}{2}^+, (\frac{11}{2}^-)$
1256.78±0.06	0.4 ±0.1	7.8	$\frac{11}{2}^+, (\frac{13}{2}^-)$
1341.5 ±0.04	0.06±0.02	8.5	
1432.29±0.23	0.37±0.04	7.7	
1503.98±0.15	0.46±0.04	7.6	$\frac{5}{2}^-, \frac{7}{2}^-$
1546.02±0.10	0.16±0.02	8.0	
1572.50±0.11	0.47±0.04	7.5	
1583.13±0.10	0.15±0.02	8.0	
1629.74±0.09	0.27±0.02	7.7	$\frac{9}{2}^+, \frac{11}{2}^-$
1654.09±0.12	0.27±0.02	7.7	$(\frac{9}{2}^-)$
1677.01±0.21	0.02±0.01	8.8	
1690.32±0.15	0.03±0.01	8.6	
1709.92±0.22	0.52±0.04	7.4	
1717.35±0.16	0.13±0.01	8.0	
1764.09±0.23	0.58±0.05	7.3	
1765.32±0.10	0.31±0.03	7.6	
1844.53±0.11	1.9 ±0.1	6.8	
1853.87±0.22	0.13±0.02	8.0	
1874.01±0.09	0.8 ±0.1	7.1	$(\frac{9}{2}^-)$
1942.49±0.13	0.4 ±0.1	7.4	
2010.18±0.20	0.39±0.03	7.4	$(\frac{5}{2}^-)$
2062.43±0.20	0.19±0.02	7.7	
2107.24±0.12	0.9 ±0.1	6.9	$(\frac{9}{2}^-)$
2142.82±0.13	1.1 ±0.1	6.9	

TABLE IV. (Continued.)

Level energy (keV)	β branching (%)	Logft	J^π
2274.06±0.07	0.7 ±0.1	7.0	
2363.54±0.24	0.05±0.01	8.0	
2382.73±0.19	0.22±0.02	7.4	$\frac{9}{2}^+, \frac{11}{2}^-$
2394.60±0.15	0.23±0.02	7.4	
2449.89±0.16	0.13±0.01	7.6	
2874.68±0.15	0.36±0.04	6.8	
2972.66±0.19	0.16±0.01	7.1	
3004.55±0.17	0.25±0.02	6.9	
3031.95±0.23	0.32±0.03	6.8	
3043.04±0.21	0.22±0.02	6.9	
3078.43±0.21	0.22±0.02	6.9	
3087.6 ±0.3	0.46±0.04	6.6	
3099.51±0.19	0.18±0.02	7.0	
3111.98±0.19	0.36±0.03	6.6	
3120.36±0.11	2.2 ±0.1	5.9	$(\frac{5}{2}^-)$
3132.88±0.20	0.32±0.03	6.7	
3170.20±0.19	0.33±0.03	6.6	
3189.67±0.15	1.3 ±0.1	6.0	
3243.04±0.17	0.51±0.04	6.4	
3247.40±0.15	0.58±0.05	6.3	
3259.26±0.20	0.31±0.03	6.6	
3273.5 ±0.3	0.59±0.04	6.3	$(\frac{5}{2}^-)$
3315.53±0.21	0.41±0.03	6.4	
3334.89±0.18	0.17±0.02	6.8	
3431.73±0.24	0.12±0.01	6.9	
3441.7 ±0.3	0.16±0.02	6.7	
3456.54±0.24	0.23±0.02	6.5	
4239.1 ±0.3	0.23±0.02	5.6	$\frac{5}{2}^+, \frac{7}{2}^+, \frac{9}{2}^+$
4364.40±0.17	0.27±0.03	5.3	$\frac{5}{2}^+, \frac{7}{2}^+, \frac{9}{2}^+$
4533.42±0.21	0.26±0.02	4.9	$\frac{5}{2}^+, \frac{7}{2}^+, \frac{9}{2}^+$
4544.72±0.22	0.20±0.02	5.0	$\frac{5}{2}^+, \frac{7}{2}^+, \frac{9}{2}^+$
4591.20±0.21	0.08±0.01	5.3	$\frac{5}{2}^+, \frac{7}{2}^+ \frac{9}{2}^+$
4671.0 ±0.3	0.19±0.02	4.7	$\frac{5}{2}^+, \frac{7}{2}^+ \frac{9}{2}^+$

by about 10^4 from those of other $N=85$ isotones to alter the assignment of $\frac{7}{2}^-$ for the 55.0-keV level.) With this assignment the 48.5-keV level can only be $\frac{5}{2}^-$.

This justification of the assigned J^π values of the three low-energy states in ^{141}Ba is made without recourse to extrapolation of level-energy systematics of the other $N=85$ isotones. The fact that the assignments agree with level systematics was certainly not surprising since this study was motivated by such considerations. Rather, this fact serves to further strengthen the case for the similar structure of these levels in the known $N=85$ isotones.

B. J^π assignments to other levels

Spin-parity assignments to other levels in ^{141}Ba can be made on a tentative basis. In addition to the usual strong argument that, with very few exceptions, all observed γ rays are of dipole or electric quadrupole multipolarity, a "missing-$E2$ transition" argument can be used for γ rays to the low-lying $\frac{3}{2}^-$, $\frac{5}{2}^-$, and $\frac{7}{2}^-$ states. Among these triplets in the $N=85$ isotones, all $E2$ transitions have comparable $B(E2)$ values, as discussed earlier. All $E2$ transitions within the triplet are observed unless their intensities are strongly suppressed by the E_γ^5 factor. This is just what is expected if all three states have the composition of "quasi-$f_{7/2}$" state,[1,2] in which the main terms in the wave functions include both $(\nu f_{7/2}{}^3)$ and $(\nu f_{7/2}{}^3)\otimes 2^+$, where the 2^+ refers to an effective quadrupole vibration of the core.[1] In the detailed analysis of Paar *et al.*[2] for ^{147}Sm, terms such as $(\nu f_{7/2}{}^2 p_{3/2})$ and $(\nu f_{7/2}{}^2 p_{3/2})\otimes 2^+$ also contribute significantly, particularly to the $\frac{3}{2}^-$ state. Thus both theory and experiment point toward considerable mixing of zero- and one-phonon terms in the triplet of low-lying states and the consequent enhancement of $E2$ transitions among them.

The mixing of terms in the wave functions of the low-lying $\frac{3}{2}^-$, $\frac{5}{2}^-$, and $\frac{7}{2}^-$ states allows a relatively strong "missing-$E2$ transition" argument to be made as follows: For levels above the low-lying triplet, any missing transition to one or more members of the triplet implies that an $E2$ transition is not possible. By this argument, levels that decay only to the $\frac{7}{2}^-$ (55 keV) level must be $\frac{11}{2}^-$, levels that decay to both the $\frac{7}{2}^-$ (55 keV) and $\frac{5}{2}^-$ (48 keV) levels must be $\frac{9}{2}^-$, and levels that decay to both the $\frac{3}{2}^-$ (ground state) and $\frac{5}{2}^-$ (48 keV) levels must be $\frac{1}{2}^-$. Levels with J^π values of $\frac{3}{2}^-$, $\frac{5}{2}^-$, $\frac{7}{2}^-$ must decay to all three members of the low-lying triplet. For this argument to be valid, there should be no exceptions such as levels that decay only to the $\frac{5}{2}^-$ member or decay to the $\frac{3}{2}^-$ and $\frac{7}{2}^-$ but not the $\frac{5}{2}^-$ member. Inspection of the level scheme in Fig. 5 shows that there are no exceptions. Furthermore, the neighboring isotones ^{143}Ce and ^{145}Nd also have no exceptions to this missing-$E2$ argument.[22,23]

Spin-parity values have been assigned tentatively by this argument to several levels in the decay scheme. Exceptions to this rule would occur for $E1$ transitions. Thus the $\frac{11}{2}^-$ level at 643 keV could instead be $\frac{9}{2}^+$ and the $\frac{9}{2}^-$ levels at 610 and 747 keV could instead be $\frac{7}{2}^+$. Furthermore, a level which decays to the $\frac{3}{2}^-$ ground state and $\frac{5}{2}^-$ state at 48.5 keV could be $\frac{3}{2}^+$ instead of the $\frac{1}{2}^-$ choice from the missing-$E2$ argument. However, positive parity states other than $\frac{1}{2}^+$, $\frac{3}{2}^+$, $\frac{5}{2}^+$, or $\frac{13}{2}^+$ are not observed experimentally at energies below ~ 1.5 MeV for $N=85$ isotones. For level energies $\gtrsim 1.5$ MeV, we have retained positive-parity possibilities as well as the negative-parity possibilities allowed by the missing-$E2$ transition argument. Transitions populating excited states have also been used to further limit possible J^π values. Spin-parity assignments or possible ranges of values are presented in Table IV.

C. Comparison with β-strength function measurements

The β-strength function measurement of Aleklett *et al.*[27] for the decay of ^{141}Cs compares quite favorably with our decay scheme. Their 0.25-MeV discriminator level prevented observation of the $\sim 57\%$ β branch at 55 keV, thus comparison is restricted to the remaining $\sim 43\%$. Aleklett *et al.* deduced peaks and valleys in S_β, the β strength function, which, although broadened by their NaI(Tl) detector resolution, corresponds well with our deduced β intensities. They deduced peaks located at excitation energies of 0.7, 1.2, and 3.2 MeV, a broad valley between ~ 1.5 and ~ 2.5 MeV, and a slowly increasing β intensity to levels above ~ 4 MeV. Our β intensities, if combined into bins of ~ 0.2 MeV width, yield the same pattern. The only exception is the level at 1844 keV, which has a β branch of $\sim 2\%$. This discrepancy may not be significant if this single level were to receive a significant amount of feeding from many weak, unobserved γ rays. The good agreement between the β intensity patterns deduced from the two measurements indicates that the cumulative effect of the intensities of unobserved γ rays from high-lying levels can have only a minor impact on our decay scheme. High-lying levels fed by β decay of $\frac{7}{2}^+$ ^{141}Cs should be predominately $\frac{5}{2}^+$, $\frac{7}{2}^+$, and $\frac{9}{2}^+$ levels, which

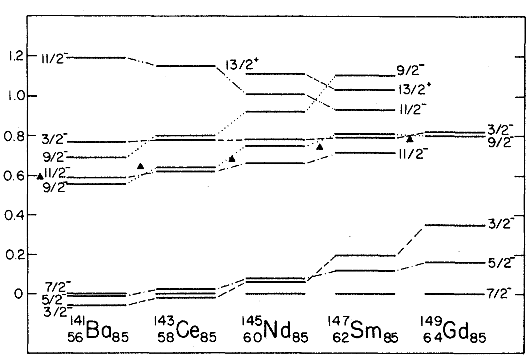

FIG. 6. Level systematics for selected levels in $N=85$ isotones. Triangles indicate the 2^+ energy in the neighboring even-even $N=84$ nuclei. Level energies are given relative to the first $\frac{7}{2}^-$ state.

decay predominately by high-energy $E1$ γ transitions to lower-energy negative-parity levels. The β branching to our levels grouped around 3.2 MeV, which totals $\sim 7\%$ of the β decay, should thus be affected only slightly by any unobserved γ rays.

V. DISCUSSION

A. Systematic trends for $N=85$ isotones

Level systematics for selected levels in $N=85$ isotones are given in Fig. 6. The levels shown in Fig. 6 were selected to emphasize the "quasi-$f_{7/2}$" nature[1,2] of these nuclides. Except for the unique-parity $\frac{13}{2}^+$ levels and possibly the second-excited $\frac{11}{2}^-$ levels, the levels, according to the analysis of Paar et al.[2] for ^{147}Sm, are predominantly formed from the three-neutron clusters $f_{7/2}{}^3$ and $f_{7/2}{}^2p_{3/2}$ together with quadrupole-phonon states based on such clusters. Before proceeding to discuss this CVM analysis in the next subsection, the systematic trends in level energies and pertinent reaction or decay data are briefly discussed.

Although the smooth trends are apparent in Fig. 6, certain features are worthy of specific comment. The energy difference between the second $\frac{3}{2}^-$ state and the $\frac{7}{2}^-$ state is nearly constant at 800 ± 20 keV. The energy difference between the first $\frac{11}{2}^-$ and the $\frac{5}{2}^-$ state is also nearly constant at 590 ± 10 keV. The first $\frac{9}{2}^-$ and $\frac{11}{2}^-$ states very closely follow the 2^+ energy of the $N=84$ isotones. The second $\frac{11}{2}^-$ states exhibit a trend with Z contrary to the other states; however, the center of gravity of the two $\frac{11}{2}^-$ states is nearly constant at 860 ± 30 keV.

Reaction studies, in particular (d,p) and $(\alpha,{}^3\mathrm{He})$ studies, have identified the $\frac{13}{2}^+$ states at 1112 and 1031 keV in ^{145}Nd (Ref. 28) and ^{147}Sm,[2,24] respectively. These states have significant $\nu f_{7/2}{}^2 i_{13/2}$ structure, although contributions from $\nu_{7/2}{}^3\otimes 3^-$ could be expected, in analogy with the situation for the $N=83$ isotone ^{147}Gd, as will be discussed later. The $\frac{13}{2}^+$ states have not been identified in β-decay studies from $\frac{7}{2}^+$ β^- decay or $\frac{1}{2}^+$ β^+ decay parents nor in (n,γ) studies, hence are not identified in ^{141}Ba, ^{143}Ce, or ^{149}Gd.

For excitation energies below about 1.5 MeV, reaction studies show that only the $p_{3/2}$ and, to a lesser extent, the $h_{9/2}$ neutron single-particle states have significant contributions to the negative-parity levels in Fig. 6. The $f_{5/2}$ and $h_{11/2}{}^{-1}$ strengths occur between 1.5 and 2.5 MeV.[22–24,28,29] For ^{143}Ce, ^{145}Nd, and ^{147}Sm, various reaction studies[22–24,28,29] have shown that most of the $p_{3/2}$ strength lies in the second-excited $\frac{3}{2}^-$ states (around 800 keV in Fig. 6) with much weaker strength to the lower $\frac{3}{2}^-$ states. The contribution of $p_{3/2}$ to the lower $\frac{3}{2}^-$ state tends to increase with decreasing Z.[28,29] The lower $\frac{9}{2}^-$ states in ^{143}Ce and ^{145}Nd were observed in (d,p) studies[28,29] to have $25-30\%$ of the $h_{9/2}$ strength, whereas the second $\frac{9}{2}^-$ states have insignificant $h_{9/2}$ strength. The second $\frac{9}{2}^-$ state in ^{147}Sm has been observed only in Coulomb excitation and inelastic scattering studies.[2,24] No reaction data exist for ^{141}Ba or ^{149}Gd.

Decay studies give the population of the $\frac{9}{2}^-$ and $\frac{11}{2}^-$ levels shown in Fig. 6 for ^{141}Ba, ^{143}Ce, and ^{145}Nd (present study, Refs. 23 and 22, respectively) as the β^- decay parent is $\frac{7}{2}^+$ for all three. The $\frac{9}{2}^-$ and $\frac{11}{2}^-$ levels in ^{147}Sm and ^{149}Gd are populated only weakly ($<0.05\%$) in ϵ/β^+ decays.[24,30] Only the first $\frac{9}{2}^-$ level has been observed to be directly populated in the ϵ/β^+ decay of $(\frac{11}{2}^-)$ ^{149}Tb^m (4.2 m).[31] For the levels in Fig. 6 above the low-lying triplet, only the second $\frac{3}{2}^-$ level is populated strongly by β decay and/or (n,γ) for all five isotones.

The level in ^{141}Ba at 827 keV, whose J^π value is limited to $\frac{3}{2}^-$, $\frac{5}{2}^-$, or $\frac{7}{2}^-$ by our decay study, is the likely candidate for the $\frac{3}{2}^-$ state around 800 keV in Fig. 6. The 772-keV energy difference between this level and the $\frac{7}{2}^-$ level at 55 keV agrees well with the 800 ± 20 keV difference for the heavier isotones. (Other possible $\frac{3}{2}^-$ levels in ^{141}Ba would give a sharp break in the near constancy of this energy difference).

Comparison of γ-ray intensity patterns for γ rays depopulating the $\frac{3}{2}^-$ levels around 800 keV in Fig. 6 does not contradict the assumption that these levels all have similar character. For ^{147}Sm and ^{149}Gd, the γ rays to the $\frac{3}{2}^-$ and $\frac{5}{2}^-$ members of the low-lying triplet were found to be dominantly $M1$.[24,30] If $M1$ is assumed to dominate for all five isotones, the reduced intensity ratio $B(M1,\frac{3}{2}^-\rightarrow\frac{5}{2}^-)/B(M1,\frac{3}{2}^-\rightarrow\frac{3}{2}^-)$ for the second $\frac{3}{2}^-$ levels has the values ~ 2.0, ~ 1.6, ~ 1.2, 0.9, and 0.3, respectively, for ^{141}Ba through ^{149}Gd. The Coulomb excitation study of Paar et al.[2] for ^{147}Sm showed that the second $\frac{3}{2}^-$ state has a noncollective $E2$ transition to the $\frac{7}{2}^-$ ground state in ^{147}Sm. The ratio $B(M1,\frac{3}{2}^-\rightarrow\frac{5}{2}^-)/B(E2,\frac{3}{2}^-\rightarrow\frac{7}{2}^-)$ also has a monotonic trend with Z, decreasing from 5.2 for ^{149}Gd to 1.4 for ^{141}Ba. The smooth variations with Z of these ratios indicate that no drastic changes in the wave functions of the states involved seems to occur as Z changes for $N=85$ isotones.

As stated earlier, comparisons of γ-ray intensity patterns for the $\frac{9}{2}^-$ states in Fig. 6 are limited by the lack of information on $M1/E2$ mixing and, for ^{147}Sm and ^{149}Gd, γ-ray intensity data. The first $\frac{9}{2}^-$ states in ^{141}Ba, ^{143}Ce, and ^{145}Nd all have the same value of 0.7 ± 0.1 for the upper limit to the ratio $B(E2,\frac{9}{2}^-\rightarrow\frac{7}{2}^-)/B(E2,\frac{9}{2}^-\rightarrow\frac{5}{2}^-)$. The second $\frac{9}{2}^-$ states in ^{141}Ba, ^{143}Ce, and ^{145}Nd, and the first $\frac{9}{2}^-$ state in ^{149}Gd, on the other hand, have upper limits of 6.4, 2.9, 1.4, and 4.2, respectively, for the $B(E2,\frac{9}{2}^-\rightarrow\frac{7}{2}^-)/B(E2,\frac{9}{2}^-\rightarrow\frac{5}{2}^-)$ ratio, which indicates that these $\frac{9}{2}^-$ states either have an increased $M1$ component in $\frac{9}{2}^-\rightarrow\frac{7}{2}^-$ or less-enhanced $E2$ components in $\frac{9}{2}^-\rightarrow\frac{5}{2}^-$ transitions. For ^{147}Sm, the Coulomb excitation study of Paar *et al.*[2] showed that the second $\frac{9}{2}^-$ state was more collective by a factor of 12 than the first $\frac{9}{2}^-$ state.

Trends in the $B(E2)$ ratios for the $\frac{7}{2}^-$ states are more difficult to interpret since only upper limits are available. The most significant information is the nearly constant ratio of ~ 0.7 for the first $\frac{9}{2}^-$ states in ^{141}Ba, ^{143}Ce, and ^{145}Nd. (Regardless of the amount of $M1$ contribution to $\frac{9}{2}^-\rightarrow\frac{7}{2}^-$, the $E2$ strength is clearly greater for $\frac{9}{2}^-\rightarrow\frac{5}{2}^-$ than for $\frac{9}{2}^-$ to $\frac{7}{2}^-$). The near constancy of this ratio implies similar wave functions for these three $\frac{9}{2}^-$ states. Further comparisons of the $\frac{9}{2}^-$ states, as well as other states, must be made on a model-dependent basis.

B. CVM treatment of $N=85$ isotones

Previous discussions of models applicable to $N=85$ isotones, i.e., the dressed n-quasiparticle model and the CVM, have been given in Refs. 31 (^{149}Gd) and 32 (^{145}Nd). The only detailed application of the three-neutron cluster CVM treatment has been for ^{147}Sm.[1,2] The following discussion is restricted to the latter, quantitative treatment and its potential for extrapolation to other $N=85$ isotones.

The $N=85$ isotones are characterized by the low-lying triplet of $\frac{3}{2}^-$, $\frac{5}{2}^-$, and $\frac{7}{2}^-$ states. Odd-A nuclei with $N=23$ or $Z=23$ exhibit an anomalous lowering of the $\frac{5}{2}^-$ state, which arises from the $1f_{7/2}{}^3$ configuration.[33] In these "true-$f_{7/2}$" nuclei, the $1f_{7/2}$ orbital is isolated in the 20−28 shell, as the neighboring $2p_{3/2}$, $1f_{5/2}$, and $2p_{1/2}$ orbitals appear some 3 to 5 MeV higher in the 28−50 shell. For $N=85$, the additional anomalous lowering of the $\frac{3}{2}^-$ state occurs because of the much smaller energy difference (~ 1.2 MeV) between the $3p_{3/2}$ and $2f_{7/2}$ neutrons.[1,2] Owing to this additional lowering of the $\frac{3}{2}^-$ states, the $N=85$ isotones are referred to as "quasi-$f_{7/2}$" nuclei.[1,2]

In addition to the low-lying $\frac{3}{2}^-$, $\frac{5}{2}^-$, and $\frac{7}{2}^-$ triplet, quasi-$f_{7/2}$ nuclei are also characterized, according to Paar *et al.*,[2] by $\frac{9}{2}^-$ and $\frac{11}{2}^-$ states of collective character as well as $\frac{3}{2}^-$ and $\frac{9}{2}^-$ states of noncollective character. In the CVM calculations of Paar *et al.* for ^{147}Sm, the states $|\frac{3}{2}^-\rangle_1$, $|\frac{5}{2}^-\rangle_1$, $|\frac{7}{2}^-\rangle_1$, and $|\frac{9}{2}^-\rangle_2$ (the second $\frac{9}{2}^-$ in the notation of Ref. 2) are collective in the sense that the $E2$ transitions to the $|\frac{7}{2}^-\rangle_1$ ground state are enhanced due to one-phonon contributions. The phases of the wave functions they deduced in describing their Coulomb excitation results[2] were such that these $E2$ transitions all had constructive interference from the various terms in the wave functions. The states $|\frac{3}{2}^-\rangle_2$ and $|\frac{9}{2}^-\rangle_1$ were found to have less collective (i.e., coherent) wave functions. The CVM calculations of Ref. 2 used only $f_{7/2}{}^3$ and $f_{7/2}{}^2\,p_{3/2}$ clusters and one-phonon (harmonic vibrator) states based on these clusters. Except for the $\sim 40\%$ $|(f_{7/2}{}^3)\frac{7}{2}^-\rangle$ term in $|\frac{7}{2}^-\rangle_1$, all individual terms were $\sim(10-25)\%$ or less. The largest term in $|\frac{3}{2}^-\rangle_2$ was $\sim 25\%$ $|(f_{7/2}{}^2)0\,p_{3/2},\frac{3}{2}^-\rangle$. In the absence of the particle-phonon interaction, i.e., to zeroth order,

$$|\tfrac{9}{2}^-\rangle_1 \simeq |(f_{7/2}{}^3)\tfrac{9}{2}^-\rangle$$

and

$$|\tfrac{9}{2}^-\rangle_2 \simeq |(f_{7/2}{}^3)\tfrac{7}{2}\otimes 2^+,\tfrac{9}{2}^-\rangle\ ,$$

hence

$$|\tfrac{7}{2}^-\rangle_1 \underset{\rightarrow}{E2} |\tfrac{9}{2}^-\rangle_2$$

is collective whereas

$$|\tfrac{7}{2}^-\rangle_1 \underset{\rightarrow}{E2} |\tfrac{9}{2}^-\rangle_1$$

is single-particle in character. With the ~ 0.5 MeV particle-phonon interaction strength, the two $\frac{9}{2}^-$ states are admixed and also contain $f_{7/2}{}^2p_{3/2}$ clusters and associated one-phonon couplings, thus the distinction in the $E2$ transition character is reduced in the final $|\frac{9}{2}^-\rangle_1$ and $|\frac{9}{2}^-\rangle_2$ states.

This "simple but therefore transparent version of the CVM," to quote Paar *et al.*,[2] was successful in reproducing the energies of the seven states con-

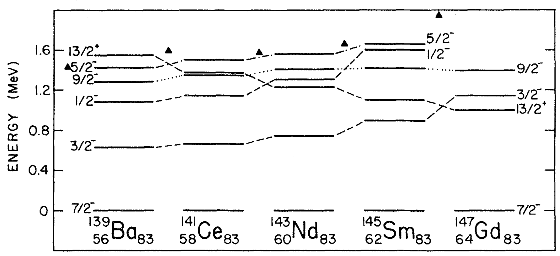

FIG. 7. Level systematics for selected levels in $N=83$ isotones. Triangles indicate the 2^+ energy in the neighboring even-even $N=82$ nuclei.

sidered and the $B(E2)$ values obtained from their Coulomb excitation study of ^{147}Sm. The dominant character of the two $\frac{3}{2}^-$ states considered agrees with reaction results[28,29] which attribute more $p_{3/2}$ strength to $|\frac{3}{2}^-\rangle_2$ than to $|\frac{3}{2}^-\rangle_1$. Omissions in this simple treatment are obvious. The $h_{9/2}$ single-particle strengths observed in the lower $\frac{9}{2}^-$ states of ^{143}Ce and ^{145}Nd, as well as the second $\frac{11}{2}^-$ states shown in Fig. 6, are outside the model space used in Ref. 2. Hopefully, the CVM treatment could be extended to include these features while retaining the dominant $f_{7/2}{}^3$, $f_{7/2}{}^2p_{3/2}$, and phonon couplings of the states already treated in Ref. 2.

A more significant test of the CVM treatment of the quasi-$f_{7/2}$ $N=85$ isotones would be to reproduce the systematic trends of the levels shown in Fig. 6. The core ($N=82$) quadrupole-phonon energy and the neutron quasiparticle energies for the shell-model orbitals above $N=82$, i.e., $2f_{7/2}$, $3p_{3/2}$, $3p_{1/2}$, $2f_{5/2}$, $1h_{9/2}$, and $1li_{13/2}$ are presented in Fig. 7. The quasiparticle energies are lower than the single-particle energies due to interactions with core phonons, both quadrupole and octupole. (For ^{147}Gd, Kleinheinz *et al.*[34] have shown that the $\frac{13}{2}^+$ first-excited state consists primarily of $\nu f_{7/2}\otimes 3^-$, where the 3^- first-excited state in ^{146}Gd lies at 1579 keV). In the quadrupole-phonon CVM calculation of Paar *et al.*[2] for ^{147}Sm, a 1.0-MeV phonon energy was used and single-particle energies were taken to be $\epsilon(f_{7/2})=0$, $\epsilon(p_{3/2})=1.2$, $\epsilon(h_{9/2})=1.5$, $\epsilon(p_{1/2})=1.6$, $\epsilon(i_{13/2})=1.7$, and $\epsilon(f_{5/2})=2.0$ MeV. The 1.0-MeV phonon energy used for ^{147}Sm was lower than the 2^+ core energy of 1.6 MeV in order to account for additional polarization of the core.[1]

The levels shown in Fig. 7 allow one to qualitatively extrapolate the ^{147}Sm calculation to lighter isotones. The 2^+ energy in the $N=82$ core nuclides is nearly constant at 1.6 MeV, except for ^{138}Ba. A phonon energy $\hbar\omega$ of 1.0 MeV is an average value for medium-heavy nuclei.[2] (A higher phonon energy is likely for ^{149}Gd, with "doubly magic" ^{146}Gd as a core.) According to Ref. 1, both the particle-vibration coupling strength a and the vibrational charge $e^{\rm vib}$ are proportional to $[B(E2,2^+\rightarrow 0^+)_{\rm core}]^{1/2}$. Since $B(E2)\simeq 0.05\ e^2b^2$ for the $N=82$ core nuclides ^{138}Ba to ^{144}Sm, the values $a\simeq 0.5$ MeV and $e^{\rm vib}\simeq 2.5e$ should be good zeroth-order estimates for all $N=85$ isotones, not just ^{147}Sm. Thus only small variations in the phonon parameters should be expected in extrapolating the CVM treatment of Ref. 2 from ^{147}Sm to lighter isotones.

Since the phonon parameters are expected to be nearly constant for ^{147}Sm and lighter $N=85$ isotones and a global pairing interaction is used for a residual pairing interaction,[2] the trends in the $N=85$ level structures should be caused mainly by changes in the single-particle energies used in the CVM treatment. The trends in quasiparticle energies shown in Fig. 7 are clearly consistent with this. As Z decreases, the $p_{3/2}$ quasiparticle energy also decreases, whereas the $h_{9/2}$ quasiparticle energy changes very little. It is anticipated that only the $f_{7/2}$, $p_{3/2}$, and $h_{9/2}$ orbitals play a significant role in the $N=85$ levels shown in Fig. 6, except for the $\frac{13}{2}^+$ level and perhaps the second $\frac{11}{2}^-$ level. The major effect of changing Z thus should be the $p_{3/2}$ quasiparticle energy. As it decreases with decreasing Z, the admixtures of terms involving the cluster $f_{7/2}{}^2p_{3/2}$ and one-phonon states based on this term should increase. This increased mixing should lead to increased $E2$ strength in γ transitions from the second $\frac{3}{2}^-$ states to the low-lying triplet. In particular, the observed decrease with Z of the ratio $B(M1,\frac{3}{2}^-\rightarrow\frac{5}{2}^-)/B(E2,\frac{3}{2}^-\rightarrow\frac{7}{2}^-)$ would follow.

The situation with the $\frac{9}{2}^-$ states is not simple to extrapolate from ^{147}Sm to lighter isotones. As discussed earlier, the two $\frac{9}{2}^-$ states in ^{147}Sm were characterized as collective (second $\frac{9}{2}^-$) and noncollective (first $\frac{9}{2}^-$).[2] The admixing of the zeroth order wave functions $|(f_{7/2}{}^3)\frac{9}{2}^-\rangle$ and $|(f_{7/2}{}^3)\frac{7}{2}\otimes 2^+,\frac{9}{2}^-\rangle$ depends on the amount of $f_{7/2}{}^2p_{3/2}$ as well as the strength of the particle-phonon interaction. As discussed in Ref. 2 the two $\frac{9}{2}^-$ states can undergo a crossover as these parameters vary, with the lower energy $\frac{9}{2}^-$ state becoming the more collective $\frac{9}{2}^-$ state. Such a crossover would be expected as Z decreased if either the $p_{3/2}$ energy drops or the particle-phonon interaction strength increases. The trends in $B(E2)$ ratios for the $\frac{9}{2}^-$ levels could be indicative of a crossover occurring around ^{145}Nd. The "evidence" for this would be apparently greater collectivity of the $\frac{9}{2}^-$ states whose ratio limits for

$$B(E2,\tfrac{9}{2}^- \to \tfrac{7}{2}^-)/B(E2,\tfrac{9}{2}^- \to \tfrac{5}{2}^-)$$

are $\sim$0.7. Thus for ^{141}Ba, ^{143}Ce, and ^{145}Nd the first $\frac{9}{2}^-$ state is the more collective one, whereas for ^{147}Sm and ^{149}Gd the second $\frac{9}{2}^-$ state is more collective. [For ^{149}Gd, the 1085-keV level, designated as $(\frac{5}{2}^-, \frac{7}{2}^-, \frac{9}{2}^-)$ in Ref. 30, which also has a $B(E2)$ ratio limit of $\sim$0.7, could be the second $\frac{9}{2}^-$ state in this isotone.] With this speculative designation of $\frac{9}{2}^-$ states in terms of their collectivity as defined in Ref. 2, the collective $\frac{9}{2}^-$ states are those with lower values ($\sim$0.7) for

$$B(E2,\tfrac{9}{2}^- \to \tfrac{7}{2}^-)/B(E2,\tfrac{9}{2}^- \to \tfrac{5}{2}^-)$$

whereas the noncollective $\frac{9}{2}^-$ states are those with $B(E2)$ ratio limits of 6.4, 2.9, 1.4, and 4.2 for ^{141}Ba, ^{143}Ce, ^{145}Nd, and ^{149}Gd, respectively. The minimal value occurs for ^{145}Nd, which is nearest to the crossover, hence where the distinction between the two types of $\frac{9}{2}^-$ characters is minimal. The noncollective $\frac{9}{2}^-$ states are the $\frac{9}{2}^-$ states whose energies change only slightly with Z, remaining near the noncollective second $\frac{3}{2}^-$ states around 0.8 MeV.

The preceding discussion of the character of the $\frac{9}{2}^-$ states in the $N=85$ isotones is speculative, since the $B(E2)$ ratios, being only limits, provide no direct support but are only indirectly supportive in that they do not contradict this designation of $\frac{9}{2}^-$ character in the $N=85$ isotones. This designation is based on a qualitative extrapolation, via the CVM calculation of Ref. 2, of the characteristics of ^{147}Sm to other $N=85$ isotones.

A far better understanding of the nature of the levels below $\sim$1 MeV would result from the quantitative extension of the CVM calculations to include all five $N=85$ isotones. Sufficient information exists on levels in these isotones, as well as the $N=82$ core and $N=83$ single-neutron nuclides, to enable a more thorough analysis of the experimentally revealed systematic trends. The adequacy of the CVM framework would be subjected to a far more severe test than the partial test provided by a single isotone such as ^{147}Sm.

ACKNOWLEDGMENTS

The non-BNL users are pleased to acknowledge the hospitality of the Neutron Nuclear Physics Group, the Physics Department, and the High Flux Beam Reactor staff during the duration of these experiments. The assistance of C. Stone, S. Faller, and C. Aras with the calibration and analysis of the lifetime data is acknowledged. The support of the U. S. Department of Energy for the laboratories and departments participating in this work is gratefully acknowledged. The strong efforts of the technical staff at TRISTAN during these experiments and during the development of the facilities is appreciated, as in the software and hardware work by Dr. M. Stelts, and H.-I. Liou, and V. Manzella.

---

*Permanent address: Institut für Kernphysik, KFA Jülich, D-5170 Jülich, West Germany.

†Permanent address: Nuclear Research Center, Negev, Beer-sheva, Israel.

[1]V. Paar, in *Proceedings of the International Conference on the Structure of Medium-Heavy Nuclei, Rhodos, 1979,* edited by the "Demokritos" tandem Accelerator Group, Athens (The Institute of Physics, Bristol, 1980); Inst. Phys. Conf. Ser. 49, 53 (1980).

[2]V. Paar, G. Vanden Berghe, C. Garrett, J. R. Leigh, and G. D. Dracoulis, Nucl. Phys. A350, 139 (1980); J. Kownacki, Z. Sujkowski, E. Hammaren, E. Liukkonen, M. Piiparinen, Th. Lindblad, H. Ryde, and V. Paar, *ibid.* A337, 464 (1980).

[3]T. Alväger, R. A. Naumann, R. F. Petry, G. Sidenius, and T. D. Thomas, Phys. Rev. 167, 1105 (1968).

[4]T. Tamai, J. Takada, R. Matsushita, and Y. Kiso, J. Nucl. Sci. Technol. 9, 378 (1972).

[5]D. Otero, A. N. Proto, and F. C. Iglesias, Phys. Rev. C 13, 1996 (1976).

[6]J. W. Cook and W. L. Talbert, Jr. (private communication).

[7]J. K. Tuli, Nucl. Data Sheets 23, 529 (1978).

[8]R. Neugart, F. Buchinger, W. Klempt, A. C. Mueller, E. W. Otten, C. Ekström, and J. Heinemeier, Proceedings of the 5th International Conference on Hyperfine Interactions, Berlin, Germany, 1980.

[9]C. Ekström, J. Heinemeier, G. Wannberg, Proceedings of the 7th International Workshop on Gross Properties of Nuclei and Nuclear Excitations, Hirschegg, Kleinwalsertal, Austria, 1979.

[10]R. G. Clark, L. E. Glendenin, and W. L. Talbert, Jr., Proceedings of the Third International Atomic Energy Symposium of the Physics and Chemistry of Fission, Rochester, 1973 (IAEA, Vienna, 1974); IAEA Proc. Ser. 2, 221 (1974).

[11]J. A. Morman, W. C. Shick, Jr., and W. L. Talbert, Jr., Phys. Rev. C 11, 913 (1975).

[12]C. Ekström, Proceedings of the Fourth International Conference on Nuclei Far from Stability, Helsingør, Denmark, 1981, CERN Report 81-09, 1981, p. 2.

[13]J. C. Hill, F. K. Wohn, R. L. Gill, D. A. Lewis, and R. E. Chrien, *Proceedings on the International Conference on Nuclear Spectroscopy of Fission Products, Grenoble, France, 1979;* edited by T. von Egidy (The Institute of Physics, Bristol, 1980); Inst. Phys. Conf. Ser. 51, 53 (1980).

[14]R. E. Chrien, M. L. Stelts, V. Manzella, R. L. Gill, F. K. Wohn, and J. C. Hill, *Proceedings on the International Conference on Nuclear Spectroscopy of Fission Products, Grenoble, France, 1979;* edited by T. von Egidy (The Institute of Physics, Bristol, 1980); Inst. Phys. Conf. Ser. 51, 44 (1980).

[15]M. Shmid, R. L. Gill, G. M. Gowdy, and C. Chung, Bull. Am. Phys. Soc. 26, 594 (1981).

[16]R. L. Gill, M. L. Stelts, R. E. Chrien, V. Manzella, H. Liou, and S. Shostak, Nucl. Instrum. Methods 186, 243

[17]J. H. Scofield, Phys. Rev. 179, 9 (1969).

[18]F. Rösel, H. M. Fries, K. Alder, and H. C. Pauli, At. Data Nucl. Data Tables 21, 91 (1978).

[19]W. Bambynek, B. Crasemann, R. W. Fink, H.-U. Freund, H. Mark, C. D. Swift, R. E. Price, and P. Venugopala Rao, Rev. Mod. Phys. 44, 716 (1972).

[20]K. D. Wünsch, R. Decker, H. Wollnik, J. Münzel, G. Siegert, G. Jung, and E. Koglin, Z. Phys. A 288, 105 (1978).

[21]F. K. Wohn and W. L. Talbert, Jr., Phys. Rev. C 18, 2328 (1978).

[22]J. K. Tuli, Nucl. Data Sheets 29, 533 (1980).

[23]J. K. Tuli, Nucl. Data Sheets 25, 603 (1978).

[24]B. Harmatz and W. B. Ewbank, Nucl. Data Sheets 25, 113 (1978).

[25]G. E. Holland, Nucl. Data Sheets 19, 337 (1976).

[26]S. Raman and N. B. Gove, Phys. Rev. C 7, 1995 (1973).

[27]K. Aleklett, G. Nyman, and G. Rudstam, Nucl. Phys. A246, 425 (1975).

[28]D. L. Hillis, C. R. Bingham, D. A. McClure, N. S. Kendrick, Jr., J. C. Hill, S. Raman, J. B. Ball, and J. A. Harvey, Phys. Rev. C 12, 260 (1975).

[29]L. Lessard, S. Gales, and J. L. Foster, Jr., Phys. Rev. C 6, 517 (1972).

[30]S. V. Jackson, J. W. Starner, W. R. Daniels, M. E. Bunker, and R. A. Meyer, Phys. Rev. C 18, 1840 (1978).

[31]K. S. Toth, E. Newman, C. R. Bingham, A. E. Rainis, and W.-D. Schmidt-Ott, Phys. Rev. C 11, 1370 (1975).

[32]S. V. Jackson and R. A. Meyer, Phys. Rev. C 13, 339 (1976).

[33]A. de Shalit and I. Talmi, *Nuclear Shell Theory* (Academic, New York, 1963), p. 348.

[34]P. Kleinheinz, J. Styczen, M. Piiparinen, M. Kortelahti, and J. Blomqvist, Proceedings of the Fourth International Conference on Nuclei Far from Stability, Helsingør, Denmark, 1981, CERN Report 81-90, 1981, p. 542.